Nanomechanics of Organic Layers and Biomenbranes

Gerard Oncins Marco

Universitat de Barcelona

Facultat de Química

Departament de Química Física

NANOMECHANICS OF ORGANIC LAYERS AND BIOMEMBRANES

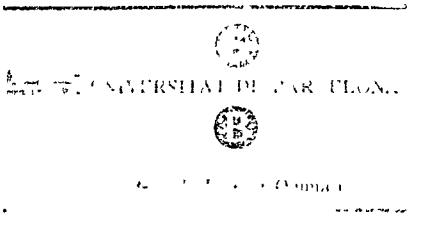

Gerard Oncins Marco

TESI DOCTORAL

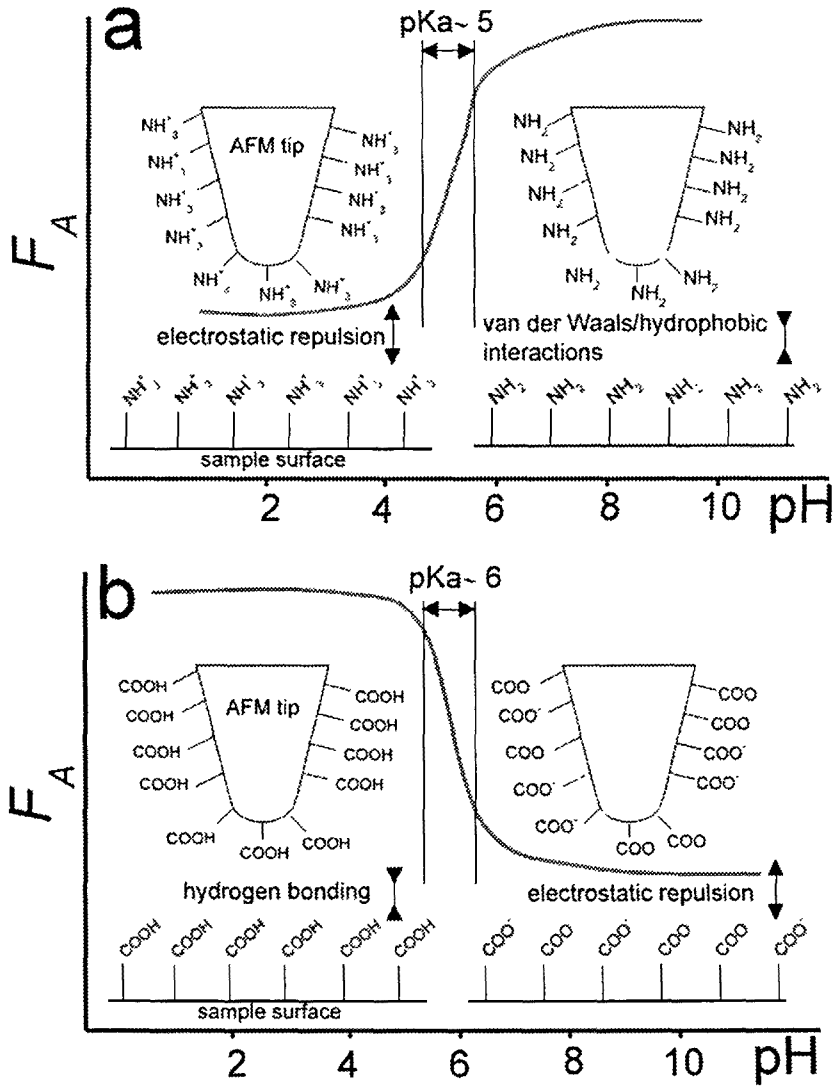

Fig. 40. Chemical Force Microscopy experiments to detect the different interactions arisen between surfaces as a function of pH[337]. F_A value is obtained from the retraction plot of Δx vs. Δz curves performed on the sample surface ands is represented as a grey line. a) At low pH values, amine functionalized surfaces and tips are protonated (repulsive interaction, low adhesion), while for pH >5, amine groups deprotonate and van der Waals and hydrophobic interactions dominate, which results in an F_A value increment. b) For –COOH functionalized tips and surfaces, hydrogen bonding between tip and sample at pH<6 results in high F_A values, which decrease for higher pH values because of carboxylic acid groups deprotonation. For both experiments, F_A vs. pH curves can be used as classical titration curves so as to calculate the pKa of the molecules.

while the liposomes become positive at higher *I* values. Having in mind that COOH functionalized tips pKa is around 5[345], it is clear that at neutral pH conditions the acidic groups will be deprotonated , rendering a negatively charged tip surface. As you may realize, the system carboxy-terminated tip and PC bilayer

is extremely interesting so as to probe a vast array of electrostatic interactions, as we can modulate the bilayer charge changing I value and the tip charge modifying the pH conditions. According to I variations at neutral pH, the authors reported that at high I values (positive bilayer), the approaching Δx vs. Δz curve shows a clear *jump-to-contact*, while for low I values (negative bilayer) the interaction is repulsive.

When the pH value is modified, the PC headgroup phosphate moiety can be protonated/deprotonated and the tip charge can be reversed. Then, from pH 10.7 to 5.0, the authors obtain a repulsive interaction in the approaching Δx vs. Δz curves, interpreted as an electrostatic repulsion arisen by the negatively charged tip and bilayer surfaces. Reducing the pH to 4.0 results in almost no-interaction, as the sample keeps on being negatively charged because of the carboxylic acid protonation. At pH 3-4, there is an acute *jump-to-contact*, which is interpreted by the authors as the tip being slightly positively charged while the sample is still negative. Around pH 3, the bilayer is neutral while the tip is slightly positive, so the interaction reduces again. Garcia-Manyes et al. also studied the adhesive region, finding that there is a sharp F_A increase around pH 3-4, corroborating the results obtained in the Δx vs. Δz approaching curves analysis.

5.3.3 Temperature. Phase transition

5.3.3.1 Phase transition. From micro- to nano-

Phospholipid bilayers undergo important structural changes depending on several factors as I or pH but perhaps temperature is the one that alters more dramatically the functionality and morphology of phospholipid bilayers and, consequently, cellular membranes[346-348]. Several different phases have been detected, being the gel (L_β) and liquid-crystalline phases (L_α) the most studied as they are involved in the phospholipid bilayer main transition event[349]. This transition is extremely important in terms of biological relevance, as it is believed that most membranes remain in the L_α phase because of its fluidity and balanced

mechanical properties[350,351]. As you may expect, acquiring a complete understanding about the changes membranes undergo as phase transitions take place is one of the cornerstones of biophysics and one of the main objectives of this thesis.

The classical way to study phase transitions is by means of Differential Scanning Calorimetry (DSC) measurements, which provide excess specific heat vs. temperature graphs were the transition events are observed as sharp heat increments at T_M[352]. It is important to note that these measurements are performed in solution, so the phospholipids are in the form of liposomes and not SPBs. In the case of PCs, Chernik[353] released a comprehensive review about the topic but, because it is more in line with the goals of this thesis, I would like to comment on the work of Sturtevant et al.[354], who studied the T_M dependence with NaCl and $CaCl_2$ concentration. By now, I would like you to have a clear idea of the effect of electrolytes in bilayers: they create ionic nets and improve the molecular packing, increasing the mechanical resistance of the whole structure. Then, Sturtevant et al. experimentally proved that the presence of NaCl or $CaCl_2$ shifts T_M to higher values, specifically from 24ºC in pure water to 26.5ºC at 5M NaCl and up to 49ºC (!) at 2M $CaCl_2$. Nevertheless, it was Yang et al.[355] who took the DSC measurements a step further into the nanoworld with a really original work; in order to explore the transition of SPBs, they incubated microscopic mica chips with DPPC liposomes and introduced the so-formed SPBs in the DSC chamber in an aqueous solution. Surprisingly, they do not observed only 1 transition, but 3 of them. To begin with, they identified the T_M of DPPC liposomes (40.4ºC) and hypothesized that the other two, which occurred at higher temperatures, corresponded with the melting of the individual phospholipid leaflets that form the SPB (Fig. 41). Assuming a weak interaction between leaflets[356-358] and that they are not surrounded by the same environment, they proposed that the low temperature transition corresponded with the outer leaflet (the one in contact with the solution), while the high temperature transition corresponded to the leaflet in contact with the

substrate, stabilized by the interaction with mica. It was time for the AFM to unveil the mystery.

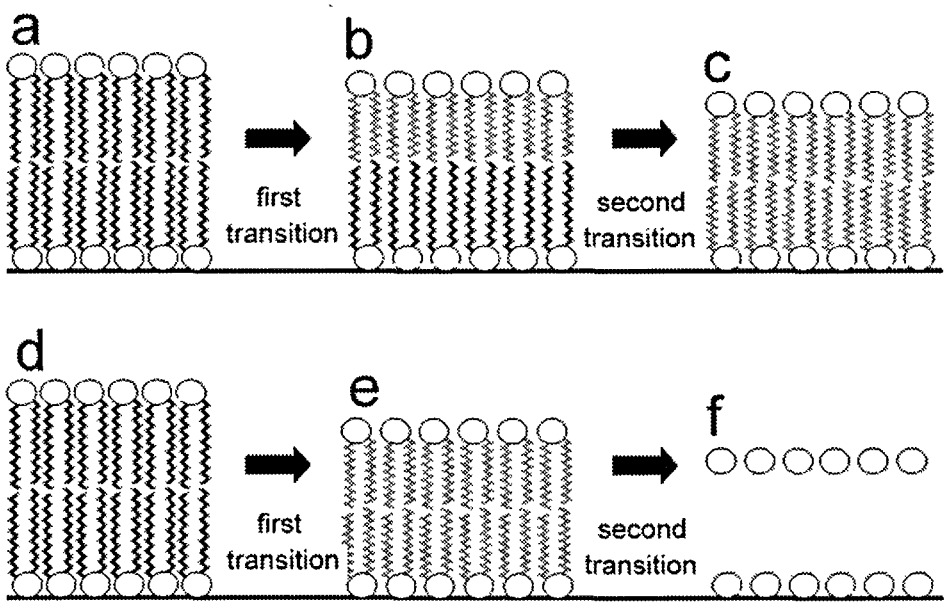

Fig. 41. 2 different proposed models to explain the two individual and consecutive transitions that are observed during the main transition event for PC phospholipids. a), b) and c) Yang et al.[355] model. a) The bilayer is entirely in the L_β phase. b) The outer monolayer melts into the L_α phase while the inner monolayer (in contact with the substrate and therefore stabilized) remains in the L_β phase. c) Both leaflets are in the L_α phase. d), e) and f) Leonenko et al. model[359]. d) Bilayer in the L_β phase. Bilayer entirely in the L_α phase. Bilayer entirely in a liquid disordered phase. Both models explain the bilayer thickness decrease observed in the topographic AFM images as main phase transition takes place.

5.3.3.2 Variable temperature AFM. In-situ transition imaging is possible.

The first application of Variable Temperature AFM[360,361] to the study of phase transitions was performed by Giocondi et al.[362] in 2001, so you can imagine that the technique is still in the development stage. They imaged 1,2-distearoyl-sn-glycero-3-phosphocholine (DSPC) and DMPC mixtures from room temperature up to 41°C so as to detect the transition from L_β to (L_β + L_α) phases as predicted by phase diagrams[363,364]. They were able to observe that for increasing temperatures below T_M, the bilayer defects (in the form of holes) closed rendering a flat and uniform surface while for temperatures higher than T_M, a lower phase that covered

a surface area that increased with temperature appeared in the image. In fact, it was the first in-situ observation of a phase transition and the authors were able to compare macroscopic thermodynamic values and Monte Carlo simulations with the real thing. There were noticeable differences, as expected, although no prove was obtained of the two transitions proposed by Yang et al.[355] in their DSC experiments. Tokumasu et al.[365] studied the transition of pure DMPC, finding that between 23°C and 27°C the DMPC bilayers reduce their thickness from 4.3 to 3.4 nm, which was in close agreement with previous X-ray measurements that reported similar thickness values for L_β and L_α DPPC phases. Besides, the transition process was proved to be reversible and it was observed that the L_α phase molecular area is higher than that of the L_β phase (the bilayer holes observed in the L_β phase closed when the bilayer was heated up to the L_α phase), which explains the thickness reduction observed in AFM topographic images. Seantier et al.[366] studied the DMPC and DPPC transitions observing similar results but introducing some interesting concepts; they claimed that the total sample thickness (5-6 nm) was not only due to the bilayer but also to a thin water film deposited between the bilayer and the mica (Fig. 32*d*), which must be taken into account because it modifies the fluidity of the SPBs and, consequently, their mechanical properties[367]. They also reported that the effect of the substrate is responsible for the T_M shifting to slightly lower temperatures[368,369] and that it also provokes a T_M range broadening. As the thoughtful reader will note, the two transitions observed in the DLC experiments should had to be detected in the in-situ imaging experiments but, so far, only one had been observed. The mystery was solved by Leonenko et al.[359], who imaged two transitions while studying DPPC bilayers supported on mica, noting that the two events extended over broad temperature ranges (42°-52°C and 53°-60°C) and were reversible. The whole transition process was observed as follows: 1) Coexistence of L_β phase with another lower phase (L_α'). 2) Disappearance of the L_β phase. 3) Coexistence of the L_α' and L_α phases. 4) Homogeneous L_α phase. They explained the broadening of the phase transition ranges as an effect of the mica support, which reduces the cooperativeness of the transition. This explanation makes sense with the SPBs transition being at higher temperatures than for liposomes (41°C[370])

but is in clear contradiction with the results presented by Seantier[366]. Interestingly, Leonenko proposed that the first observed transition corresponds with the main L_β to L_α transition and the second, with the formation of a fluid-disordered phase where the hydrocarbon phospholipid chains are interdigitated (this phase forms the thinnest bilayers) as depicted in Fig. 41. Concerning the nanomechanics of these bilayers, Leonenko observed that F_A on Δx vs. Δz curves performed on the L_β phase is smaller and less reproducible than that obtained on fluid phases (L_α' or L_α). They suggested that the number of phospholipid molecules that interact with the tip in a fluid phase is higher than in a solid phase, which explains the F_A difference, and that the higher mobility of the fluid phase increases the membrane homogeneity, with the consequent F_A reproducibility increment. Besides, they compared their F_A values with the energy to remove a single phospholipid molecule from a bilayer (around 100 pN[371,372]), concluding that the each Δx vs. Δz curve retraction process involves molecular patches with more than three phospholipid molecules[373].

Charrier et al.[374] Performed similar experiments on DMPC, observing the three phases present in the main phase transition, which for SPBs is a double process (there was no doubt by then). They refined the measurements and observed that it was possible to finely control the bilayer structure playing with temperature and that the three observed phases were stable. In order to explain the nature of the double main transition, they proposed that the two phospholipid leaflets underwent separate transitions from the L_β to the L_α phase, as it had been proposed by Yang[355]. Besides, they observed that the transitions were shifted to higher temperatures for SPBs respect to liposomes in solution and explained the fact in terms, not only of the stabilization due to the substrate presence but also of the different bilayer surface tension according to the structure shape (spherical in the case of liposomes and planar in the case of SPBs). They proposed a model in the framework of the van't Hoff theory[375,376] to explain both the transition shifting and the transition temperature range broadening in the case of SPBs. Similar results were reported by Keller et al.[377], who observed that the inner monolayer transition temperature range is much narrower than that of the outer monolayer and that the two processes do

not overlap, that is, the outer leaflet melts in first place and when it is in the L_α phase, the process begins in the inner leaflet. According to these results they proposed that the melting of the outer leaflet is a prerequisite for the inner monolayer to melt, as it is stabilized by the electrostatic interactions between the PC polar heads and the mica surface and the consequent polar moieties dehydration state. Besides, the outer monolayer, which is not affected by the mica surface, has a similar transition enthalpy to that measured for free standing liposomes[377].

Despite all the work done, there are still some questions that need to be answered. To begin with, two different mechanisms have been proposed until now in order to explain the two consecutive transitions observed in the main transition process. Despite all the theoretical work and hypothesis, there is still no evidence about which is the correct one (if any!). In this sense we performed some experiments with DPPC monolayers that we believe shed some light on this question and that can be found in the experimental section. Besides, there is no a clear idea about which is the phase transition mechanism. How does the bilayer melt? Do they begin the phase transition in the defects or perhaps in the grain boundaries? Again, some answers can be found in the experimental section.

5.4 EXPERIMENTAL RESULTS

5.4.1 Effect of Ion-Binding and Chemical Phospholipid Structure on the Nanomechanics of Lipid Bilayers Studied by Force Spectroscopy

S. Garcia-Manyes, G. Oncins, F. Sanz

Department of Physical Chemistry, Universitat de Barcelona, Spain

Biophysical Journal 89, (2005), 1812-1826

5.4.1.1 Summary

This work deals with the effect that cations play in the stability of phospholipid bilayers. The effect of ions in the polar moieties of these molecules had been observed in the past by means of z-potential and DSC measurements but there was no evidence of the effect of ions on supported bilayers. In this sense, this work presents Force Spectroscopy measurements on different phospholipid bilayers both in L_β and L_α phases. The obtained F_y values are considered as nanomechanical fingerprints of the tested bilayers due to the sensitivity of this mechanical figure of merit to the nanostructure of the samples.

The obtained results can be summarized as follows:

- *The phospholipid SPBs break under the exertion of a certain F_y and the total P_d during the penetration event corresponds with the bilayer thickness.*

- *The shape of the F_v vs. P_d curves can be explained as a function of the DLVO interactions between tip and sample and the mechanical properties of the bilayer. Besides, the mechanical model developed by some of the authors of this work in a previous paper proves to be suitable to explain the contact mechanics between the bilayer and the tip.*

- *The F_v value increases with the NaCl concentration for a certain bilayer. This can be explained considering that ions increase the compactness of the bilayer by creating an ionic network with the polar heads and promoting the van der Waals interactions between the phospholipid hydrocarbon chains.*

1812 Biophysical Journal Volume 89 September 2005 1812–1826

Effect of Ion-Binding and Chemical Phospholipid Structure on the Nanomechanics of Lipid Bilayers Studied by Force Spectroscopy

Sergi Garcia-Manyes, Gerard Oncins, and Fausto Sanz
Department of Physical Chemistry, Universitat de Barcelona, Barcelona Spain

ABSTRACT The nanomechanical response of supported lipid bilayers has been studied by force spectroscopy with atomic force microscopy We have experimentally proved that the amount of ions present in the measuring system has a strong effect on the force needed to puncture a 1,2-dimyristoyl-*sn*-glycero 3 phosphocholine bilayer with an atomic force microscope tip, thus highlighting the role that monovalent cations (so far underestimated, e g Na^+) play upon membrane stability The increase in the yield threshold force has been related to the increase in lateral interactions (higher phospholipid-phospholipid interaction, decrease in area per lipid) promoted by ions bound into the membrane The same tendency has also been observed for other phosphatidylcholine bilayers, namely, 2-dilauroyl-*sn*-glycero-3-phosphocholine, 1 2-dipalmitoyl-*sn*-glycero-3-phosphocholine, and 1,2 dioleoyl-*sn*-3 phosphocholine and also for phosphatidylethanolamine bilayers such as 1-palmitoyl 2 oleoyl *sn*-3-phosphoethanolamine Finally this effect has been also tested on a natural lipid bilayer (*Escherichia coli* lipid extract), showing the same overall tendency The kinetics of the process has also been studied, together with the role of water upon membrane stability and its effect on membrane nanomechanics Finally, the effect of the chemical structure of the phospholipid molecule on the nanomechanical response of the membrane has also been discussed

INTRODUCTION

The physical and chemical properties of biological membranes are crucial to understanding membrane functions The main biological role of bilayers is to provide a barrier that divides electrolytic solutions into different compartments Therefore the effect of electrolytic solutions on membranes is of great importance and has generated wide research (1) Besides, ion binding affects the stability of proteins and their process of binding to membranes (2), and it is also mainly responsible for lipid vesicle fusion (3,4)

From an experimental point of view, many works, especially in the 1980s, have dealt with the quantification of membrane surface potential through the electrophoretic mobility of lipid membranes under solutions with different ionic strength, allowing the calculation of the ζ potential value (5,6) More recently, contributions regarding infrared (2) and fluorescent techniques have also helped to shed light on this issue Finally, recent molecular dynamics (MD) simulations have allowed us to understand the underlying processes from an atomistic point of view and have helped us to study the role that cations play upon membrane structure and stability (7–9) Between the experimental macroscopic techniques and the theoretical atomistic approaches to this issue, atomic force microscopy (AFM) has proved to be a powerful technique that has allowed imaging of surfaces with subnanometric resolution This technique has helped us to understand how supported planar lipid bilayers (SPBs) assemble and what the interaction forces are that act between vesicle and substrate surfaces and also between membrane surfaces, which is fundamental to efforts in chemistry, structural biology, and biophysics (10,11)

SPBs have been used as model membranes to study cell-cell recognition in the immune system, adhesion of cells, phospholipid diffusion, protein binding to lipid ligands, and membrane insertion of proteins (12,13) By imaging lipid bilayers in aqueous media with AFM, both molecular structure and morphological aspects have been demonstrated (14–17) Besides, the force spectroscopy mode allows us to obtain valuable experimental information about the mechanics of the systems with nanometric and nanonewton resolution In recent years, force spectroscopy has been applied to the study of nanomechanical properties of different systems including nanoindenting hard surfaces (18,19) or cells (20), studying the solvation forces near the surfaces (21,22), dealing with the interactions of chemically functionalized probes and surfaces (so called chemical force microscopy) (23,24), or unfolding protein molecules (25,26) Thanks to these force measurements, valuable information can be obtained regarding phospholipid interaction forces such as those generated by either Derjaguin Landau Verwey Overbeek (DLVO) forces, hydration forces, or steric forces (27) Recent contributions have dealt with membrane nanomechanics using force spectroscopy, especially regarding measurement of the elastic/plastic behavior of the bilayer as a function of its composition, or the interaction with chemically modified probes (16,27,28)

Concerning the force curves on lipid bilayers, some authors have described jumps on the approaching curve, this breakthrough being interpreted as the penetration of the AFM tip through the lipid bilayer (29) The force at which this jump in the force plot occurs is the maximum force the bilayer is able to withstand before breaking Therefore,

Submitted April 5 2005 and accepted for publication June 7 2005

Address reprint requests to Fausto Sanz Dept of Physical Chemistry Universitat de Barcelona 1 11 Martí i Franquès 08028 Barcelona Spain Tel 34 934021240 Fax 34 934021231 E mail fsanz@ub edu

0006 3495/05/09/1812/15 $2 00

doi 10 1529/biophysj 105 064030

a quantitative measurement of the force at which the jump occurs can shed light on basic information concerning cell membrane nanomechanics as well as interaction forces between neighboring lipid molecules in the membrane. Some of the factors (variables) involved in membrane stability can be assessed through this jump in the force plot thanks to those force spectroscopy measurements. Likewise, the force at which this jump occurs can be regarded as a "fingerprint" of the bilayer stability under the experimental conditions in which the measurement is performed, just as force is the fingerprint for a protein to unfold or for a hard material surface to be indented. Controlling the involved variables can result in a better understanding of the regulating processes that nature can use to govern cell membrane interactions.

So far, the main reported variables for breakthrough dependence are 1), temperature (phase); 2), tip chemistry and phospholipid chemistry; and 3), tip approaching velocity. Concerning temperature, although there is much debate about whether the jump can be observed in both the gel and liquid phases or only in the gel phase, little is known experimentally about this dependence except for a report in a recent publication (30) in which it is posited that the breakthrough force decreases as the temperature increases. Regarding tip chemistry and phospholipid chemistry, it has been demonstrated that although hydrophilic tips yield a high material-dependent breakthrough force, hydrophobic tips give rise to a breakthrough force near the contact force (28). Finally, the greater the tip approaching velocity, the higher the force at which the jump will occur (31,32). However, even though those parameters are now being studied, there are two fundamental issues that have not yet been elucidated: 1), the effect of phospholipid chemical structure; and 2), the effect of the ionic strength of the measuring media on the yield threshold value. Regarding the former, a first approach has been reported (27,28), but there are still some questions lacking answers: Is the polar head in the phospholipid molecule the element mainly responsible for the bilayer nanomechanics or does the hydrophobic tail also play an important role? And further, does the degree of insaturation also play a role in the compactness of the bilayer?

Concerning the issue of ionic strength, we know that electrostatic interactions govern structural and dynamical properties of many biological systems (33,34). In the case of phospholipid bilayers, the role of monovalent ions (e.g., Na^+) seems to have been so far underestimated, as theoretical simulations seem to predict. Indeed, MD simulations (9,35) suggest a strong interaction between sodium and calcium ions and the carbonyl oxygens of the lipids, which thus forms tight ion-lipid complexes, giving rise to a higher degree of membrane organization. Likewise, the lateral interaction between the phospholipid molecules increases, with the overall result of a more efficient packing (reduction of the area per lipid value) of the phospholipid structure. Since natural lipid membranes are composed of different phospholipid molecules in a wide range of concentrations, it is always difficult to assess the contribution of every type of phospholipid to the total nanomechanical response of the system. The role of ionic strength can be tested on all phospholipid systems, even though for the sake of simplicity, and to start with, we first dealt with model lipid membranes such as 1,2-dimyristoyl-*sn*-glycero-3-phosphatidylcholine (DMPC), 1,2-dilauroyl-*sn*-glycero-3-phosphocholine (DLPC), and 1,2-dipalmitoyl-*sn*-glycero-3-phosphocholine (DPPC) deposited on mica. Later on, the study was extended to a phosphatidylethanolamine (PE) bilayer, and finally, the nanomechanical response of a natural lipid bilayer (*Escherichia coli* lipid extract) was studied.

The goal of this study is mainly to demonstrate an experimental, quantitative force spectroscopy detailed approach to understanding the nanomechanics of lipid bilayers and the forces involved in membrane deformation and failure in aqueous environment, especially dealing with the role of ionic strength on the nanomechanical response of the membrane. The discussion and interpretation of the results will be made in the framework of available data obtained through both theoretical calculations and experiments to correlate the changes in mechanical response of the system with the structural changes induced in the membrane upon ion binding considered from an atomic point of view. Additionally, we aim to perform a first approach to relate the chemical composition of the phospholipid molecule with its mechanical response.

MATERIALS AND METHODS

Sample preparation

DMPC (Sigma, St. Louis, MO) (>98%) was dissolved in chloroform/ethanol (3:1) (Carlo Erba, Milan, Italy, analysis grade 99.9%) to give a final DMPC concentration of 2 mM. This dissolution was kept at −10°C. A 500-μl aliquot was poured in a glass vial and the solvent was evaporated with a nitrogen flow, obtaining a DMPC film at the bottom of the vial. The solution was kept in a vacuum overnight to ensure the absence of organic solvent traces. Then, aqueous buffered solution at the correct ionic strength was added to achieve a final DMPC concentration of 500 μM containing 0 mM NaCl, 50 mM NaCl, 75 mM NaCl, 100 mM NaCl, and 150 mM NaCl + 20 mM $MgCl_2$, respectively. All solutions used in this work were set at pH 7.4 with 10 mM Hepes/NaOH. Because of the low solubility of DMPC in water, the vial was subjected to 30-s cycles of vortexing, temperature, and sonication until a homogeneous mixture was obtained. The solution was finally sonicated for 20 min (to have unilamellar liposomes) and allowed to settle overnight, always protected from light and maintained at 4°C. Before use, mica surfaces (Metahx, Madrid, Spain) were glued onto teflon discs with a water insoluble mounting wax. Fifty microliters of DMPC dissolution at the specific NaCl concentration was applied to cover a 0.5 cm^2 freshly cleaved piece of mica for a deposition time of 35 min. After that, the mica was rinsed three times with 100 μl of the corresponding ionic aqueous solution. The process of vesicle formation and deposition for the rest of the phospholipid bilayers used in this work (DLPC, DPPC, 1-palmitoyl-2-oleoyl-*sn*-3-phosphoethanolamine (POPE), and 1,2-dioleoyl-*sn*-3-phosphocholine (DOPC), all from Sigma, >98%) is the same as that described for DMPC. In the case of DPPC, however, the temperature cycles for resuspension were set to ~50°C due to the higher T_m for this phospholipid. *E. coli* lipid extract (nominally 67% phosphatidylethanolamine, 23.2% phosphatidylglycerol, and 9.8% cardiolipin), was purchased from Avanti

Polar Lipids (Alabaster AL). Basically the polar lipid extract is the total lipid extract precipitated with acetone and then extracted with diethyl ether (36). The process for vesicle formation is also the same as the one described for DMPC.

ζ-Potential measurements

ζ Potential measurements were performed with a Zetamaster Particle Electrophoresis Analyser through which the velocity of the particles can be measured with a light scattering technique by using the Doppler effect thanks to a pair of mutually coherent laser beams (5 mW He Ne laser at 633 nm). Zetamaster measures the autocorrelation function of the scattered light and after the signal processing it obtains the electrophoretic mobility and finally through the Henry equation the ζ-potential.

AFM imaging

AFM images were acquired with a Dimension 3100 (Digital Instruments Santa Barbara CA) microscope controlled by a Nanoscope IV controller (Digital Instruments) in contact mode using V shaped Si_3N_4 cantilever tips (OMCL TR400PSA Olympus Tokyo Japan). The applied force was controlled by acquiring force plots before and after every image was captured to measure the distance from the set point value.

Force spectroscopy

Force spectroscopy was performed with a Molecular Force Probe1 D (Asylum Research Santa Barbara CA). Force plots were acquired using V shaped Si_3N_4 tips (OMCL TR400PSA Olympus) with a nominal spring constant of 0.08 N/m. Individual spring constants were calibrated using the equipartition theorem (thermal noise)(37) after having correctly measured the piezo sensitivity (V/nm) by measuring it at high voltages after several minutes of performing force plots to avoid hysteresis. It should be pointed out that the results shown here for DMPC bilayers were obtained with the same cantilever keeping the spot laser at the same position on the lever to avoid changes in the spring constant calculation (38). However results have low scattering when using different tips and different samples. ~1300 curves over more than 15 positions were obtained for each sample. All force spectroscopy and AFM images were obtained at 20 ± 0.5°C, which is below the main phase transition temperature (T_m) of DMPC (23.5°C). Besides we have to consider here that T_m for supported bilayers shifts to a higher temperature than observed in solution (39). Therefore, we are indenting the gel phase for DMPC supported bilayers. Applied forces F are given by $F = k_c \times \Delta$ where Δ is the cantilever deflection. The surface deformation is given as penetration (δ) evaluated as $\delta = z - \Delta$ where z represents the piezo scanner displacement.

Chemically modified AFM probe preparation

Commercially available gold coated cantilevers (OMCL TR400PB Olympus) with nominal spring constant of $k_c = 0.09$ N/m were cleaned and placed into a 10 mM 16 mercaptohexadecanoic acid (Sigma) isopropanol solution and kept at 4°C overnight. Before use tips were rinsed with isopropanol and distilled water. Sonication was briefly applied to remove thiol aggregates that might be adsorbed. The quality of the self assembled monolayers was confirmed using contact angle measurements.

RESULTS AND DISCUSSION

DMPC model membrane

A first experimental approach to study ion adsorption on the membrane is the measurement of the liposome mobility in an electrophoretic field and likewise measuring the ζ-potential. Although the ζ-potential does not directly yield the surface charge, but the charge at the point where the Stern layer and the diffuse layer meet (shear plane), it is considered to yield a significant approximation of the surface potential. Fig. 1 shows the evolution of the ζ-potential value of a DMPC unilamellar liposome solution as the ionic strength of the solution is increased. All concentrations refer only to NaCl addition, except for the last point in the graph, in which 20 mM $MgCl_2$ have been added to a 150-mM NaCl solution to mimic physiological concentrations. As the ionic strength increases, the net ζ-potential value increases, reflecting that indeed positive cations may adsorb on the surface of the polar head of the phospholipid molecule. It is widely accepted that most natural membranes are negatively charged because of the presence of variable quantities of negatively charged phospholipids, yielding surface charges on the order of -0.05 C/m^2 (1). However, in this case, we have to take into account that even though phosphatidylcholine (PC) heads are zwitterionic and thus theoretically globally uncharged at neutral pH, it gives rise to a negative ζ-potential value (-12.0 ± 1.6 mV) in mQ water. This has been interpreted in terms of hydration layers formed around the surface (40) and to the orientation of lipid headgroups (6).

The process of vesicle fusion to flat bilayer is assumed to be electrostatically governed, and it is assumed that surface free energy plays a key role (41). Freshly cleaved mica is negatively charged upon a wide range of ionic strength (40), so that according to Fig. 1 the higher the ionic strength, the higher and the faster will be the adhesion of DMPC liposomes to the mica surface. This process will be especially favored at high ionic strength, where the surface ζ potential is positive (6.86 ± 2.3 mV). The probable divalent cation preference for membrane binding may also help to reverse the obtained net ζ-potential value (from negative to positive values). Fig. 2 shows AFM contact mode images of DMPC

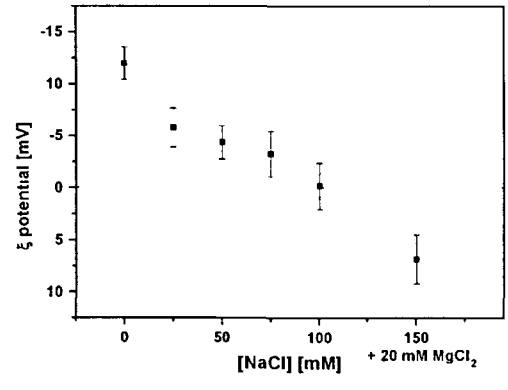

FIGURE 1 ζ Potential values of the DMPC liposomes versus ionic strength of the measuring solution. Every point in the graph is the average of 15 independent measurements. Error bars represent standard deviation values.

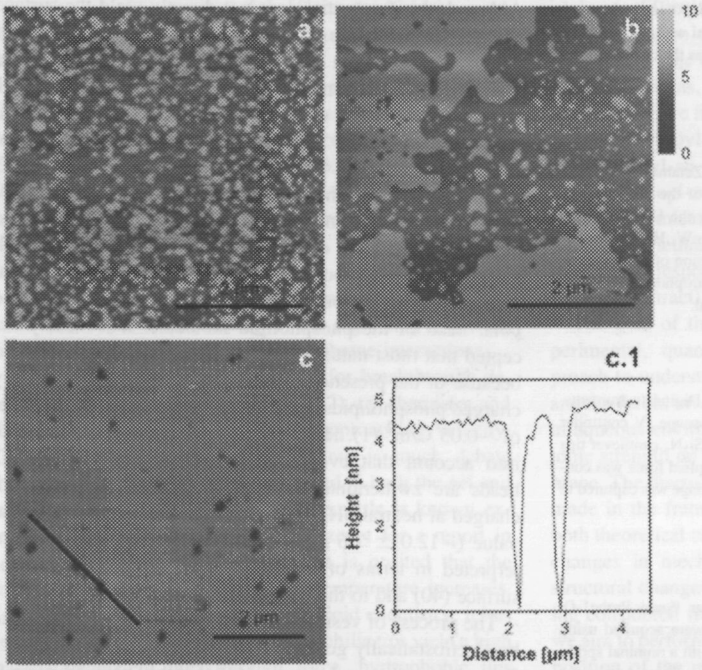

FIGURE 2 AFM contact mode images (5 × 5 μm^2) of DMPC bilayers in (*a*) distilled water, (*b*) 100 mM NaCl solution, and (*c*) AFM contact mode images (7 × 7 μm^2) of DMPC bilayers in 150 mM NaCl + 20 mM $MgCl_2$. All solutions were buffered to pH 7.4 with 10 mM Hepes/NaOH. (*c.1*) Cross-section profile of the marked area in *c*. All images were taken after 35 min of liposome deposition.

bilayers as the ionic strength of the surface is increased, showing that the degree of surface coverage is strongly dependent on the amount of ions present in the system. Fig. 2 *a* shows a 5 × 5-μm^2 contact mode image of DMPC bilayer in distilled water, Fig. 2 *b* shows the image in 50 mM NaCl, and Fig. 2 *c* shows a 7.5 × 7.5-μm^2 image of DMPC in 150 mM NaCl + 20 mM $MgCl_2$ 10. Fig. 2 *c.1* shows a cross section of the marked area in Fig. 2 *c* in which, thanks to the surface defects, the bilayer height can be measured at ~4.5 nm.

A series of 500-μM DMPC solutions in Millipore water with different ionic strengths (0 mM, 50 mM, 75 mM, and 100 mM NaCl or 150 mM NaCl + 20 mM $MgCl_2$, all with 10 mM Hepes, pH 7.4) were deposited onto a freshly cleaved mica surface and mounted on a Molecular Force Probe1-D liquid cell.

Force curves (Fig. 3) exhibit a breakthrough feature (*black arrows*) in the approaching curve corresponding to the penetration of the bilayer by the tip apex and indicating that the lipid bilayer is not able to withstand the force exerted by the tip. Concerning the retracting curve we observe an adhesion peak, which corresponds to the adhesion between the silicon nitride tip and the surface. The width of the jump (~4.5 nm) corresponds to the height of the bilayer (cross section in Fig. 2 *c.1*). In Fig. 3 *a*, the breakthrough force (also called yield threshold) occurs at ~15 nN. This curve has been taken in a solution of 150 mM NaCl + 20 mM $MgCl_2$. In Fig. 3 *b*, the force plot was taken on a DMPC bilayer in distilled water and the yield threshold is found at ~2.2 nN, which is ~7 fold lower.

Fig. 4 shows the histograms of the yield threshold force values ranging from 2.76 ± 0.11 nN in pure water to 14.93 ± 0.09 nN in buffered high ionic strength solution. Those histograms have been obtained taking only the successful indentation recordings (we call a successful recording the one that presents a breakthrough in the force plot). As we have already clearly seen in Fig. 2, the higher the ionic strength, the higher the degree of coverage of the surface. Thus, the probability of a successful recording is higher as we increase the ionic strength of the solution. In the cases in which the bilayer presents uncovered regions (e.g., Fig. 2, *a* and *b*), when an unsuccessful force plot occurs it means that we are attempting on an "empty" area, and we normally observe a typical silicon nitride-bare mica force plot. All histograms here shown belong to the same sample. However, maximum variations of 15–20% have been found between histograms in different experiments (e.g., different sample, different tip).

In Fig. 5, a graph showing the yield threshold force versus the different ionic strengths is shown. Every point in the graph corresponds to the Gaussian center of the Gaussian fit to the data of the histograms shown in Fig. 4. Clearly, the increase in ionic strength gives rise to an increase in the force required to puncture the bilayer. This dependence gives rise to a linear relationship between force and ionic strength (slope ~70 pN/mM). (To obtain this linear fit, the last point in the graph has been supposed as a first approximation to be 210 mM to account for the double charged Mg^{2+} effect.) Here we must point out that all experiments have been

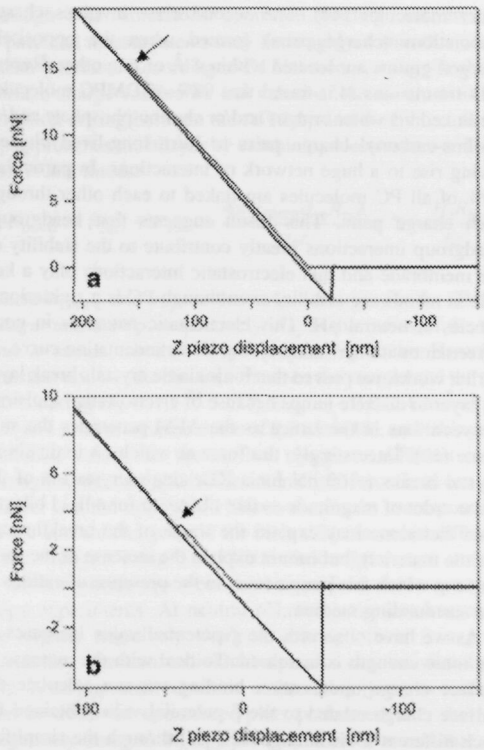

FIGURE 3 Force versus z-piezo displacement plot for a DMPC bilayer in (a) 150 mM NaCl + 20 mM $MgCl_2$ and (b) distilled water. Yield threshold is denoted by black arrows at ~15 nN (a) and ~2.1 nN (b). The width of the jump, ~4.5 nm, corresponds well with the bilayer height measured using contact mode AFM.

performed at the same indenting velocity (400 nm/s) so that the small effect of velocity on the breakthrough force would not impact the results.

It is important to point out that in a few cases a double jump in the force plots has been observed (Fig. 6). This double jump has been interpreted (42) as a second lipid bilayer that has been formed on the tip. Interestingly, we have only observed double jumps under high ionic strength conditions (~10% of the total force plots under 100 mM NaCl and ~15% of the total force plots under 150 mM NaCl + 20 mM $MgCl_2$ buffered solution); they have never been observed under lower ionic strength concentrations. Due to the slightly negatively charged silicon nitride surface (−0.032 C/m^2 at pH 7.0) (43), bilayer deposition onto the tip may be favored at high ionic strength in a process parallel to that observed for mica. Another experimental issue supporting this fact is that this second jump has never been observed when carboxyl chemically functionalized tips were used, even in the presence of high salt concentration, highlighting again the role of surface free energy upon bilayer

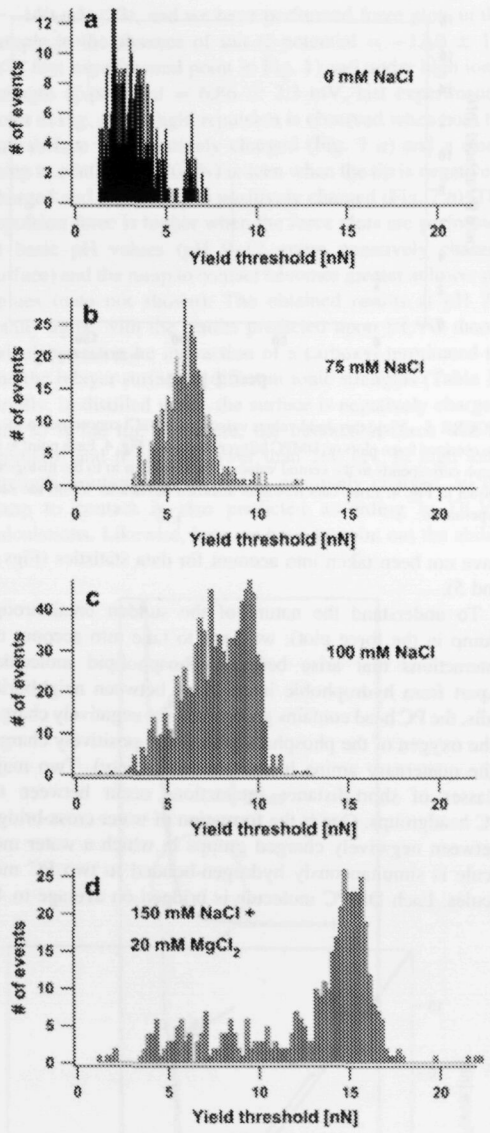

FIGURE 4 Histograms corresponding to the yield threshold force value for DMPC bilayers under different ionic compositions: (a) 0 mM NaCl, x = 2.76 ± 0.11 nN (N = 396); (b) 75 mM NaCl, x = 6.04 ± 0.04 nN (N = 568); (c) 100 mM NaCl, x = 7.98 ± 0.13 nN (N = 872); and (d) 150 mM NaCl + 20 mM $MgCl_2$, x = 14.93 ± 0.09 nN (N = 427). All results correspond to a Gaussian fitting of the data shown in the histogram. Results are presented as the Gaussian center $x \pm 2s/\sqrt{N}$.

deposition. These results are in agreement with those observed by Pera et al. (42) and Franz et al. (29), which correlated the presence of the second jump with salt concentration. The force plot recordings where two jumps have been observed

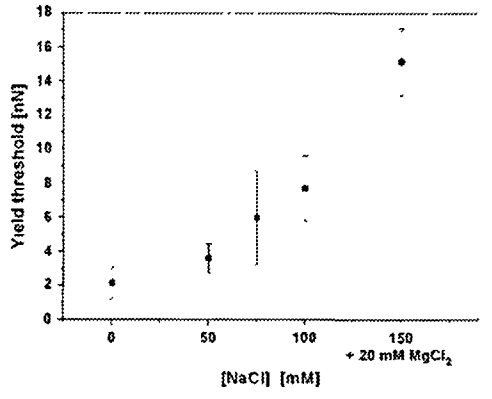

FIGURE 5 Yield threshold values versus ionic NaCl concentration for all the obtained force plots on DMPC bilayers shown in Fig. 4. Each point in the graph corresponds to the central value of the Gaussian fit to the histograms shown in Fig. 4. Error bars represent standard deviations within the same experiment.

have not been taken into account for data statistics (Figs. 4 and 5).

To understand the nature of the sudden breakthrough (jump in the force plot), we have to take into account the interactions that arise between phospholipid molecules. Apart from hydrophobic interactions between neighboring tails, the PC head contains groups that are negatively charged (the oxygen of the phosphate group) and positively charged (the quaternary amine in the choline moiety). Two major classes of short-distance interactions occur between the PC headgroups. One is the formation of water cross-bridges between negatively charged groups in which a water molecule is simultaneously hydrogen-bonded to two PC molecules. Each DMPC molecule is bridged on average to 4.5

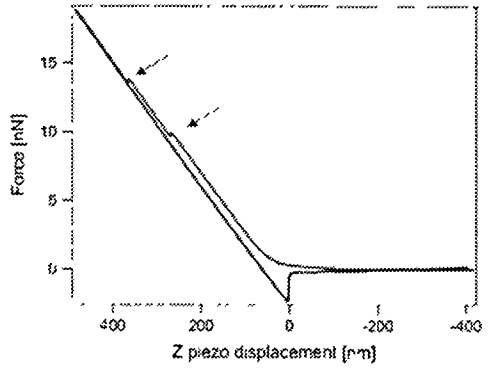

FIGURE 6 Force plot on a DMPC lipid bilayer under high ionic strength conditions (150 mM NaCl + 20 mM $MgCl_2$) where a second jump in the force plot occurs, probably due to a second lipid bilayer deposited on the silicon nitride AFM tip apex. This second bilayer may be stabilized by the presence of salt.

water molecules (44). The second class involves charge associations (charge pairs) formed when the oppositely charged groups are located within 4 Å of one other. Recent MD simulations (45) found that 98% of DMPC molecules are linked via water bridges and/or choline-phosphate and/or choline-carbonyl charge pairs to form long-lived clusters giving rise to a huge network of interactions. In particular, 90% of all PC molecules are linked to each other through such charge pairs. This result suggests that headgroup-headgroup interactions greatly contribute to the stability of the membrane and that electrostatic interactions play a key role in membrane stability even though PC is a zwitterionic species at neutral pH. This electrostatic nature is in good agreement with the sudden jump in the indentation curve. In earlier works, we proved that ionic single crystals break layer by layer in discrete jumps because of electrostatic repulsions between ions in the lattice as the AFM penetrates the substrate (19). Interestingly, the force at which an ionic single crystal breaks (~60 nN for a KBr single crystal) is of the same order of magnitude as that observed for a lipid bilayer. This fact alone may explain the shape of the breakthrough (brittle material), but cannot explain the increase of the force value at which this jump occurs in the presence of cations in the surrounding medium.

As we have observed, the ζ potential value increases as the ionic strength is increased. To deal with the increase in surface charge upon cation binding we can calculate the surface charge related to the ζ-potential value obtained for each different ionic strength (Fig. 1) through the simplified Grahame equation for low potentials (46).

$$\sigma = \varepsilon\varepsilon_0\kappa\psi_0, \qquad (1)$$

where σ stands for the surface charge, κ stands for the reciprocal of the Debye length, and ψ_0 stands for the surface potential. The surface charge values are 2.12×10^{-3} C/m^2 at 25 mM ionic strength, -1.30×10^{-4} C/m^2 at 100 mM ionic strength, and 6.89×10^{-3} C/m^2 at 150 mM NaCl + 20 $MgCl_2$. Those values are in agreement with those found in Marra and Israelachvili (47). However, they are far too low to explain the high Na^+ and Mg^{2+} coordination numbers found upon MD simulations. The surface charge calculated through the Gouy-Chapman theory assumes that the interface between the membrane and aqueous solution is planar with zero width and that the charge on the membrane is homogeneously distributed on the membrane surface in a continuous way. This assumption has proved in MD simulations to be rather dramatic in the case of a membrane/aqueous solution interface. Even in this case, simulations predict a surface potential similar to the obtained values through ζ-potential experimental measurements (Gouy-Chapman model) for distances >10 Å from the bilayer surface (8). Therefore, the Gouy-Chapman model theory describes qualitatively well the membrane/solution interface for distances >1 nm away from the "real" membrane surface. The huge discrepancy between the potential values obtained

through MD simulations upon ion binding and through ζ potential measurements may be roughly within this nanometer interface. According to DLVO theory, using the above surface charge values, we can calculate the electrostatic interaction arising between the AFM tip and the bilayer as the tip approaches the bilayer by combining electrostatic and van der Waals forces.

$$F_{DLVO} = F_{el} + F_{VdW} = \frac{4\pi\sigma_{DMPC}\sigma_{tip}R_{tip}\lambda}{\varepsilon_0\varepsilon}e^{-z/\lambda} - \frac{H_aR_{tip}}{6z^2}, \quad (2)$$

where σ_{DMPC} and σ_{tip} are the surface charges for the DMPC bilayer and the tip, respectively, R_{tip} is the radius of the tip, and λ stands for the Debye length. H_a is the Hamaker constant and z is the distance between the sample and the tip. Considering $H_a = 10^{-21}$ J (47), $\sigma_{tip} = -0.032$ C/m^2 at pH 7.0, and a mean area/molecule of 0.5 nm^2 (48), and taking the obtained values for the surface charge at different ionic strengths, we can obtain the interaction force between the bilayer and the tip. Table 1 shows the results corresponding to the surface charges and the interaction forces at different ionic strengths using bare silicon nitride tips.

Silicon nitride tips were used to perform force spectroscopy experiments. At neutral pH, those tips are known to be slightly negatively charged, although there is a great variability between individual tips. As can be seen from Fig. 3, no important repulsion or attraction (jump to contact) can be observed upon force plots performed with the low negatively charged Si_3N_4 tips. Therefore, it seems that the breakthrough force cannot be (totally) explained in terms of electrostatic interaction between tip and sample. To have chemically controlled tips (negatively charged at neutral pH), and to address the question of to what extent electrostatic interactions can play a role in the membrane breakthrough, we have functionalized gold-coated AFM tips with 16-mercaptohexadecanoic acid ($pK_a \sim 4.7$), surface potential

TABLE 1 DLVO parameters for the interaction of the AFM tip and the studied surface when the tip is bare silicon nitride or carboxyl-terminated

[NaCl] (M)	λ (nm)	σ_{tip} (C/m^2)	$\sigma_{DMPC} \times 10$ (C/m^2)	DLVO force (nN)
Silicon nitride tip				
0.025	1.92	−0.03	−2.12	0.00260
0.05	1.358	0.05	2.25	0.015
0.075	1.108	−0.06	−2.07	0.004
0.1	0.96	0.06	1.31	Attraction
0.15 + 0.02 $MgCl_2$	0.662	−0.09	6.89	Attraction
Carboxyl terminated tip				
0.025	1.92	0.15	2.12	0.26
0.05	1.358	−0.21	−2.25	0.44
0.075	1.108	0.25	2.07	0.51
0.1	0.96	−0.29	−0.134	0.089
0.15 + 0.02 $MgCl_2$	0.662	0.51	6.89	Attraction

The terms λ, σ_{tip}, and σ_{DMPC} stand for the Debye length, the tip surface charge, and the bilayer surface charge, respectively, for both tips.

~ 140 mV (23), and we have performed force plots in the sample in the absence of salt (ζ-potential 12.0 ± 1.6 mV, first experimental point in Fig. 1) and under high ionic strength (ζ-potential ~ 6.86 ± 2.3 mV, last experimental point in Fig. 1). A slight repulsion is observed when both tip and surface are negatively charged (Fig. 7 *a*) and a small jump to contact (~220 pN) is seen when the tip is negatively charged and the surface is positively charged (Fig. 7 *b*). The repulsion force is higher when the force plots are performed at basic pH values (pH 9–12, more negatively charged surface) and the jump to contact becomes greater at lower pH values (data not shown). The obtained results at pH 7.4 totally agree with the results predicted upon DLVO theory calculations for the interaction of a carboxyl-terminated tip and the bilayer surface at different ionic strengths (Table 1). Briefly, in distilled water, the surface is negatively charged, and so is the tip. Therefore, the interaction force will be repulsive and it will be lower than 260 pN. In high ionic strength solution, the surface is positively charged, so the jump to contact is also predicted according to DLVO calculations. Likewise, here we have to point out the ability

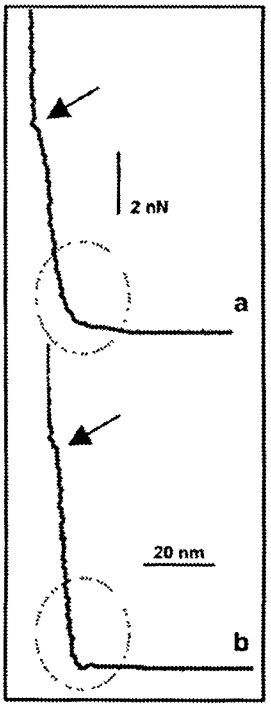

FIGURE 7 Force plots obtained as a 16-mercaptohexadecanoic acid approaches a DMPC bilayer under (*a*) distilled water, 10 mM Hepes pH 7.4, negative surface charge, and (*b*) a 150 mM NaCl + 20 mM $MgCl_2$ solution, 10 mM Hepes pH 7.1 positive surface charge. Yield threshold is indicated by an arrow.

of chemically modified tips to sense surface charges, even when they are of a few mC/m^2. In any case, the repulsive forces are <1 nN and thus in both curves the yield threshold point (*arrow*) clearly occurs at a much higher force than the electrostatic interaction force regime here presented.

Hydration and steric forces have been described as responsible for short distance repulsion between two opposing lipid bilayers. Indeed, it is the force needed to remove the water molecules adsorbed on amphiphilic groups as both surfaces come into contact (46). It has been shown that the role of water is extremely crucial to membrane stability. It is *therefore quite straightforward to think that hydration force* may play a role in membrane mechanical stability. Therefore, if water was replaced with, e.g., ethanol, the overall network created by the H-bonds would be partially disrupted and therefore one might expect that the yield threshold would be much lower (that is to say, lateral interactions between phospholipid molecules in the membrane would be reduced so that it would be easier for the tip to penetrate the membrane). Indeed, it has been reported that short-chain alkanol, such as ethanol, displaces water from the network with an overall effect of weakening lipid-lipid interactions by increasing headgroup spacing (higher area per lipid) (49). To address the question of whether this decrease in lateral interactions has any effect on the nanomechanics of the system we have formed a DMPC bilayer under water and, once formed, replaced water with an EtOH/water solution (50:50%, $x_{ethanol}$ 0.72). Immediately after the solution was added, a clear decrease in the rupture force was observed down to ~0.5 nN, as shown in Fig. 8. Interestingly, no membrane disruption was observed, since in 100% of the cases a jump (break) in the force plot was observed (if the membrane had been disrupted, the retracting curve of the force plot would have shown not a clear adhesion peak, indicating the sudden snap-off from the surface, but a continuous, nonreproducible feature that indicates that material is being pulled off the surface. In this case, when membrane is disrupted (for concentrations higher than 75.25%, ethanol/water), no jump in the extending force plot is observed since membrane is not packed enough). These results are in agreement with AFM images, in which membrane dissolution was not observed upon ethanol addition, and the only observed feature was the growing of small holes in the system, *suggesting a less compact structure. Similar results* have been obtained when the bilayer has been formed under high ionic strength. In this case, the yield threshold values both before and after ethanol addition were shifted to higher values on account of the cations present in the bilayer. It seems clear, then, that water plays a key role in membrane structure and that this fact has a direct effect on membrane mechanical deformation.

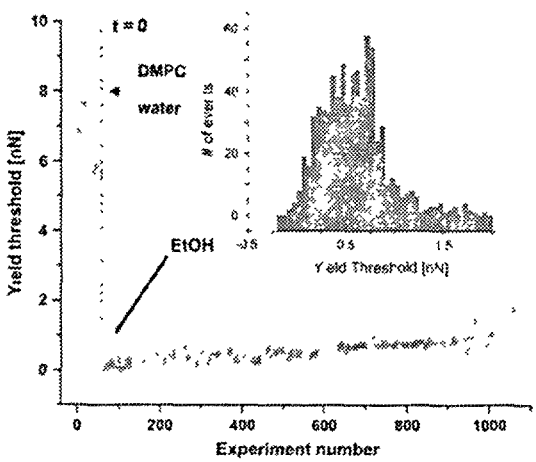

FIGURE 8 Evolution of the force at which the yield threshold occurs after the addition of a 50:50% ethanol/water solution. After addition of ethanol the yield threshold force value occurs at λ 0.533 ± 0.03 nN (N 731) (Gaussian fit to the histogram).

Hydration force has been reported (27) to extend to ~5 nN and cannot alone explain the force-distance curves acquired with AFM until the breakthrough point. This hydration force is short-ranged and follows the expression

$$F_{hydration} \quad F_0 e^{-z/\lambda}, \tag{3}$$

where F_0 is the preexponential factor, z is the separation between the surfaces, and λ is the hydration decay length. Typically, F_0 ~0.15–2 nN and λ 0.2–0.35 nm for measurements performed with a surface force apparatus (46) and 2–5 greater for measurements performed by AFM between lipid bilayers and alkanethiol-functionalized probes(27). Instead, a mechanical contribution accounting for the elastic deformation of the bilayer was needed to fully account for the force-distance shape of the curve until the plastic regime was achieved (27).

Molecular dynamics simulations have recently demonstrated (7,9,35) that the presence of cations (namely, Na^+ and Ca^{2+}) in the phospholipid network would change drastically the structural and dynamical properties of the PC membranes. On average, every Na^+ cation binds to three carbonyl oxygens and to one to two water oxygens. Due to their threefold increased size as compared to single lipids, these complexes are less mobile. As a consequence, a decrease in the average area per lipid from 0.655 nm^2 to 0.606 nm^2 (>8%) is observed for POPC, giving rise to a more compact overall structure. Indeed, the difference in the area per group is also reflected by the ordering of the lipid hydrocarbon tails (7,9). A similar case applied to Ca^{2+}, each Ca^{2+} cation binding to 4.2 PC heads on average. The same MD simulations revealed that despite those significant changes, the profile of the total electric potential across the bilayer for distances >10–18 Å from the center of the bilayer is only slightly changed due to the close distribution of Cl counterions giving rise to a strong capacitor, and especially to the fact that water molecules reorient their dipoles near the

membrane surface (distances < 10 Å). It is well known that for distances less than this, water molecules do not exhibit bulk-like properties (8). Overall, the total electric potential a nanometer away from the surface does not change as much as one would predict at first sight, and these results are in very good accordance with the (low) values obtained upon ζ-potential measurements, even when they demonstrated the same tendency to increase in value as the ionic strength is increased. Therefore, and according to those molecular dynamics simulations, the higher-order structure promoted by ions on the bilayer that give rise to a the reduction in average area per lipid (higher compactness) and to a more rigid structure (lower diffusion coefficient) may be the cause for the higher membrane stability experimentally observed through the nanomechanical response of the system obtained by force spectroscopy measurements. It seems then that rather than drastically increasing the electrostatic potential across the membrane (z direction) the introduction of ions in the membrane gives rise to a much higher lateral interaction within neighboring headgroups, with the overall result of a higher packing and compactness of the whole network composing the membrane. This increase in the lateral forces (closer distance between individual molecules) is probably the last responsible for membrane higher resistance upon breaking. This fact is in very good agreement with earlier results obtained for halide single crystal nanoindentation (19), where we demonstrated both experimentally and theoretically that the yield threshold force value was dependent on the anion cation distance in the lattice (a lower ion distance gave rise to a higher yield threshold force value, e.g., for NaCl compared to a compound, such as KBr, with higher ion-cation distance) in a single-crystal study of a series of alkali halides. To elucidate the role that those reported lateral interactions within the phospholipid network play upon membrane deformation we have applied a simple model that we proposed elsewhere (19), which takes into account the lateral interactions while the surface is being deformed by an AFM tip. Those lateral interactions are modeled by the dynamics of the deforming surface as n coupled springs. According to this model, the dependence of the surface counterforce opposing the AFM tip penetration follows the expression

$$F(\delta) = k\delta\left(1 - d_s/\sqrt{(\delta^2 + d_s^2)}\right), \tag{4}$$

where k and d_s stand for an effective spring constant equal to the Debye wavevector and the length at zero elongation, respectively. Fig. 9 shows the indentation plot of a DMPC bilayer measured in aqueous solution, 25 mM NaCl, pH 7.4, until the jump (onset of the plastic deformation) occurs. The elastic spring model (4) has been fitted to the experimental data after the first ~100 pN (electrostatic interaction) up to the yield threshold. The fit to the model is shown in Fig. 9 with a continuous shaded line. As is clear from the graph, the fit describes quite well the elastic deformation region of the indentation plot. This fit gives rise to a k value of 17.1 N/m

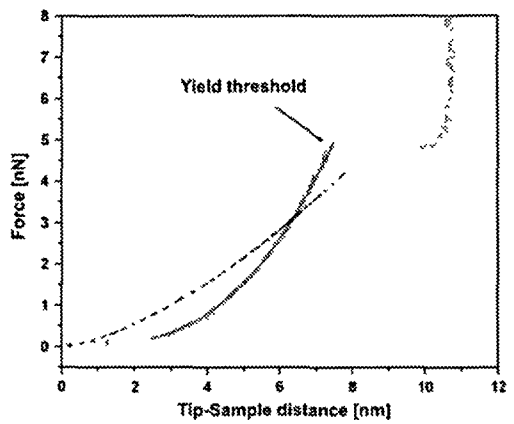

FIGURE 9 Force-distance curve corresponding to the indentation of a DMPC bilayer under 25 mM NaCl, pH 7.4. The elastic region (up to the yield threshold point) has been fitted (*a*) to the spring model (*continuous shaded line*) and (*b*) to the Hertz model, taking R = 31 nm (*dashed line*).

and a d_s value of 26.1 nm. The k value indicates the stiffness of the surface upon deformation, whereas the d_s value indicates the whole perturbed length before breaking. Interestingly, this d_s value is much higher than those found for alkali halide single crystals (d_s = 0.9 ± 0.3 nm for NaCl) indicating that deformation is a cooperative process in which many molecules are involved in the membrane deformation before breaking (the deformed area being much greater than the contact radius itself). In the case of a solid alkali halide single crystal this plastic failure occurs because the charge repulsion within the lattice is so strong that the surface is not able to deform anymore, giving rise to a brittle failure in a fast layer by-layer plastic deformation process. Besides, the ratio between the obtained k and d values gives rise to 337 MPa, which is a value similar to the reported reduced Young modulus for distearoylphosphatidylethanolamine (170 MPa). This ratio yields similar values to Young modulus values for ionic systems, but fails for nonionic (covalent) systems, suggesting that lipid bilayer deformation can be partially governed by electrostatic interactions. The simple spring model was used to describe elastic deformation of surfaces in the nanometer range after realizing that the Hertz model did not succeed in describing elastic deformation at this scale, which is not surprising since the Hertz model is a macroscopic model and its boundary conditions are not fulfilled upon indentation with an AFM tip and also since we must take into account that the substrate is relatively hard as compared to the organic layer (50). For a paraboloid indenter, the Hertz equation yields

$$F = 4/3\,E^* R^{1/2}\delta^{3/2}, \tag{5}$$

where E^* stands for the reduced Young modulus. That the elastic regime of lipid bilayers cannot be described by

the Hertz equation has been recently stressed (30). A fit of the experimental data to the Hertz model is also included in Fig. 9, taking $R \sim 31$ nm (individually measured by imaging a silicon calibration grid, Micromasch, Ultrasharp, TGG01, silicon oxide), and letting E^* be the free variable (*dashed line*). As can be easily seen, the Hertz model does not reproduce the experimental data, whereas the spring model can adjust the experimental data. Besides, an exponential-growth equation accounting for hydration forces (3) has been also applied, but the hydration decay length (λ) yields an unrealistic value of 2.8 nm. If a decay length of 0.35 nm is fixed, the equation does not reproduce the experimental data at all. Therefore, a mechanical deformation component of the bilayer seems to be the factor responsible for most of the *repulsive regime between the AFM tip and the lipid bilayer*, at least after the first nanometer separation. Similar results were reported for distearoylphosphatidylethanolamine bilayers (27).

Kinetics

The incorporation of ions into the PC headgroup can be finally proved to be a fully reversible process with relatively fast kinetics in the timescale of the experiment: a compact lipid bilayer was formed in the physiological solution (150 mM NaCl + 20 mM $MgCl_2$), we measured the yield threshold value, and, once done, we replaced the solution with distilled water. The yield threshold decreased to a value of ~6.2 ± 0.12 nN, increasing again to ~15.9 ± 0.15 nN when water was replaced with the former solution (Fig. 10). The waiting time from changing the solution and measuring was ~10 min in each case. In the same line, we studied the direct evolution of the yield threshold with time while changing the measuring solution by recording >3000 consecutive force plots in the same spot of the surface over more than 1 h (Fig. 11). Until about experiment 1200, the measuring solution was water. Then, water was removed and replaced with the former high ionic strength physiological solution. The yield threshold varied from ~3 nN to ~15 nN in ~15 min, and even though there is some scattering in the data after experiment 1750 (maybe on account of not totally homogeneous distribution of ions), a more or less stable value plateau was reached. Thus, taking into account the region between the two plateaus we can roughly assess that the kinetics of the system has a rate constant of ~0.7 nN/min. This fact indicates that the process of binding cations is not an instant process. In any case, the kinetics of the process is experimentally measurable within the AFM timescale.

So far we have proved that the ionic strength gives rise to a huge increase in the force needed by the AFM to penetrate the membrane for a DMPC bilayer. The next step is to assess whether this process takes place with other PC bilayers and also with bilayers composed of phospholipids with other zwitterionic heads.

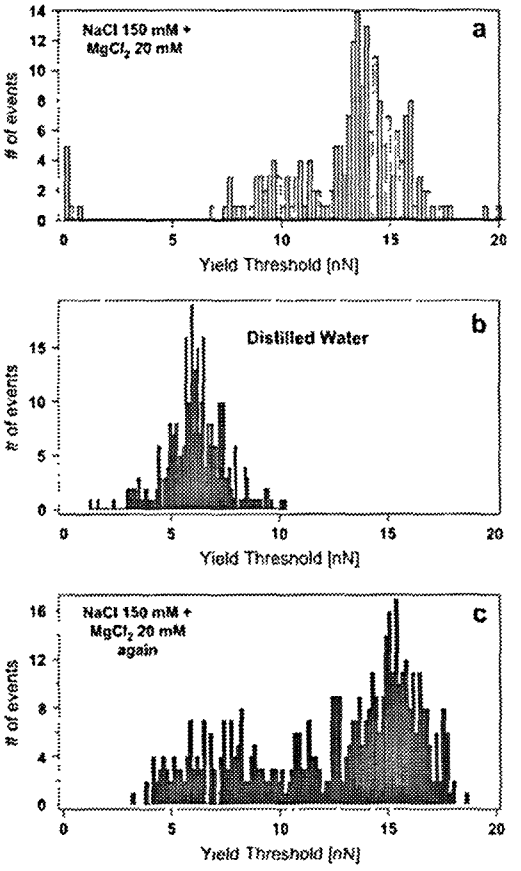

FIGURE 10 Histograms of the yield threshold force value for DMPC bilayers under different ionic strength values. (*a*) 150 mM NaCl + 20 mM $MgCl_2$, τ 14.12 ± 0.16 nN (N 350); (*b*) 0 mM NaCl, τ 6.2 ± 0.12 nN (N 328); and (*c*) 150 mM NaCl + 20 mM $MgCl_2$, τ 15.9 ± 0.15 nN (N 483). The measured bilayer is the same in all three cases. Once the bilayer is formed and measured at a high ionic strength, the solution is replaced with water, measured again, and then water is replaced with the former solution.

PC bilayers: effect of ion-binding and phospholipid chemical structure

Dealing with PC bilayers, we have performed the same experiment with DLPC and DPPC, which only differ from DMPC in the number of CH_2 groups in the fatty acid chain. Fig. 12 shows the histograms corresponding to the yield threshold value for a DLPC membrane measured in water (Fig. 12 *a*) and in high ionic strength physiological solution (Fig. 12 *b*). The yield threshold value shifts from 3.78 ± 0.04 nN in the case of water to 6.12 ± 0.08 nN for high ionic strength physiological solution. Data for DMPC measured in water (Fig. 12 *c*) and in high ionic strength physiological solution (Fig. 12 *d*) are also included for the sake of

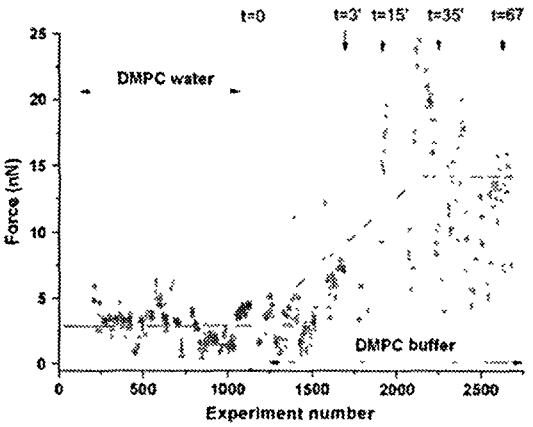

FIGURE 11 Evolution of the yield threshold force value with time in the same spot of the surface (ignoring drift) along an experiment in which water was replaced with high ionic strength solution (*dotted line*). Then time was set to zero as high ionic strength solution was added. After ~ 15 min a more or less stable plateau is reached. The orange line is meant to guide the eye.

comparison. Similarly, Fig. 12, *e* and *f*, shows the histogram for DPPC measured in water and in high ionic strength physiological solution, respectively. Again in this case the effect of ionic strength (*I*) is clear, since the breakthrough force is 7.02 ± 0.06 nN when measured in water solution and 20.31 ± 0.29 nN when measured at high ionic strength. Fig. 12 *h* shows the change in ζ-potential value as the ionic strength of the medium is increased from 0 mM (distilled water) to 100 mM NaCl for four different PC liposomes, namely DLPC, DMPC, DPPC, and DOPC. In all cases, the higher the ionic strength, the higher (less negative) the ζ-potential value, meaning that in all cases there is adsorption of monovalent cations in the membrane, which can be again easily correlated with the nanomechanics of the systems (Fig. 12, *a–f*). In light of these results, in which phospholipids with the same headgroup (PC) and different chain length have been studied, the effect of the chemical structure of the phospholipid tail on the nanomechanical response of the bilayer can also be addressed. The comparison of the yield threshold force values obtained for the previous PC bilayers, i.e., DLPC (12:0), DMPC (14:0), and DPPC (16:0), where numbers in parentheses represent number of carbon atoms in the fatty acid chain per number of insaturations (Fig. 12, *a–f*), are summarized in Fig. 12 *i*, where the relationship between the yield threshold force value and the number of carbon atoms present in the fatty acid of the phospholipid molecule composing the bilayer is shown. Dark squares stand for the measurements performed under high ionic strengths (Fig. 12, *b*, *d*, and *f*) and white squares stand for the measurements performed in distilled water (Fig. 12, *a*, *c*, and *e*). According to Fig. 12 *i*, the effect of ionic strength on the nanomechanics of the system is evident for the three PC phospholipids studied. However, this effect is especially outstanding in the case of DMPC and DPPC (yielding a yield threshold force value increment, ΔF_y, between the measurements obtained under high ionic strength and those obtained under distilled water of ~11 nN in the case of DMPC and ~14 nN in the case of DPPC). This yield force value increment is smaller in the case of DLPC (ΔF_y ~3 nN). This result could be interpreted in terms of the phase in which the different phospholipids are present. Although DLPC (T_M = −1°C) is in the liquid phase at 20°C, DMPC (T_M = 24°C) and DPPC (T_M = 42°C) are both in the gel phase at this temperature. Therefore, these results suggest that although ion binding has influence on both the gel phase and the liquid phase, it is in the gel phase that this effect is more enhanced. We have recently addressed the effect of temperature on the yield threshold value of lipid bilayers in a systematic study that corroborates these results (S. Garcia-Manyes, G. Oncins, and F. Sanz, unpublished). When comparing the nanomechanical response of the bilayer for the two phospholipids present in the gel phase (DMPC and DPPC) we realize that the longer the tail, the harder it is to puncture the membrane, yielding an increase of ~5 nN for every two extra CH_2 groups present in the hydrophobic tail in the case of measurements performed under high ionic strength and an increase of ~4 nN in the case of measurements performed in distilled water. In this case, where phospholipids are in the same (gel) phase, these differences become a direct measurement of van der Waals interactions between phospholipid neighboring tails. Those results experimentally demonstrate that the length of the hydrophobic chains of the phospholipid molecules indeed have an influence on the nanomechanics of the system. A systematic study concerning the individual effect of the hydrophilic headgroup and the hydrophobic tail for different phospholipids, both charged and zwitterionic, all in the same phase, is an ongoing experiment in our laboratory. Finally, the role of the insaturations in the fatty acid has also been taken into account. We have studied the mechanical response of DOPC (18:1), in which, although the 18 carbon atoms in the chain may predict a higher yield threshold value than DPPC, the insaturation in the chain gives rise to a lower overall packing of the molecule (~30° tilting), clearly yielding a lower resistance to rupture than expected (Fig. 12 *g*), although it is found in the liquid-like phase. The influence of the insaturation degree and also of the stereochemistry of the insaturation (whether this is in the *cis* or *trans* conformation) will also be interesting for future research in this area.

POPE bilayer

To check whether the effect of ion-binding on the mechanical response of the membrane found in PC bilayers is also observed in other zwitterionic phospholipid headgroups, such as PE, we have measured the yield threshold values with two different salt concentrations for a POPE bilayer.

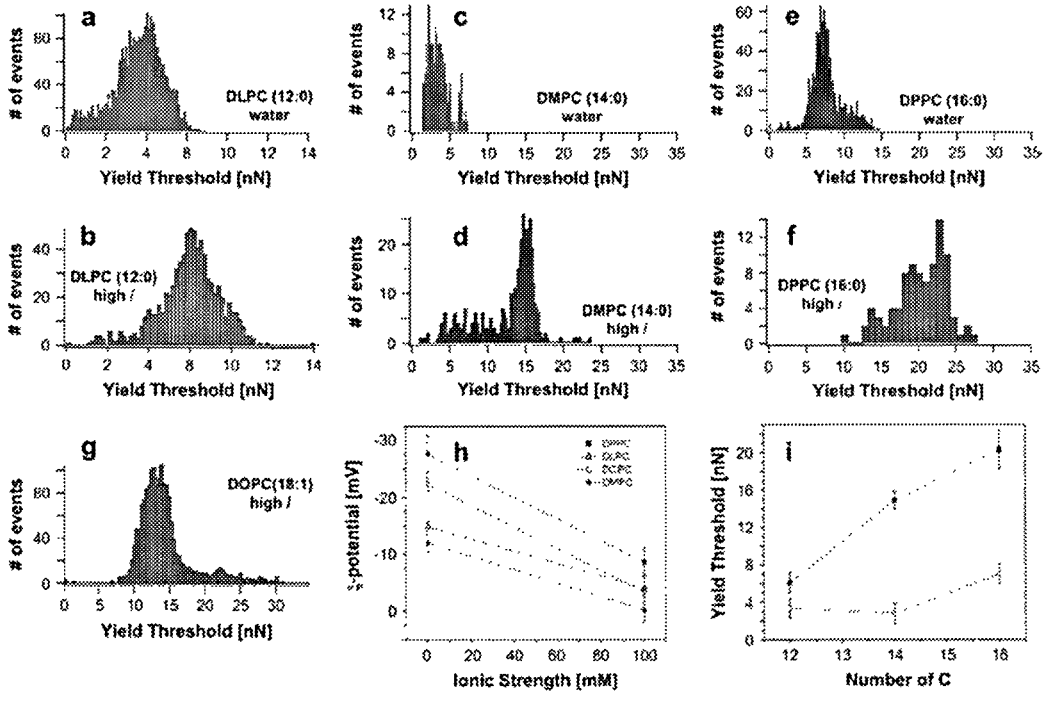

FIGURE 12 (*a* and *b*) Histograms of the yield threshold value for DLPC in water and 150 mM NaCl + 20 mM $MgCl_2$, respectively, where (*a*) $x = 3.78 \pm 0.04$ nN ($N = 2650$) and (*b*) $x = 6.12 \pm 0.08$ nN ($N = 791$). (*c* and *d*) Histograms of the yield threshold value for DMPC in water and 150 mM NaCl + 20 mM $MgCl_2$, respectively, where (*c*) $x = 2.76 \pm 0.11$ nN ($N = 396$) and (*d*) $x = 14.93 \pm 0.09$ nN ($N = 427$). (*e* and *f*) Histograms of the yield threshold value for DPPC in water and 150 mM NaCl + 20 mM $MgCl_2$, respectively, where (*e*) $x = 7.02 \pm 0.06$ nN ($N = 1272$) and (*f*) $x = 20.31 \pm 0.29$ nN ($N = 785$). (*g*) Histogram of the yield threshold force value for DOPC (18:1), where $x = 14.4 \pm 0.10$ nN ($N = 1691$). All results correspond to a Gaussian fitting of the data shown in the histogram. Results are presented as the Gaussian center $x \pm 2s/\sqrt{N}$. (*h*) ζ-Potential values of the PC liposomes as the ionic strength increases. Every point in the graph is the average of 15 independent measurements. Error bars stand for standard deviation value within the measurement. Lines are a guide to the eye. (*i*) Dependence of the yield threshold value for the studied saturated PC as a function of the carbon atoms present in the fatty acid chain. Black squares represent measurements performed under high ionic strength conditions and white squares represent measurements performed in distilled water. Error bars are standard deviations of the measurement. Lines are a guide to the eye.

The same tendency observed with PC is observed with PE despite the different chemical structure of the head. At 50 mM NaCl the yield threshold takes place at 1.63 ± 0.03 nN and increases to 3.43 ± 0.04 nN when measured in a 100 mM NaCl solution. The low yield threshold values compared to those observed for PC phospholipids can be explained in terms of the chemical difference of the headgroup, the chain unsaturation, the phase in which POPE is found at 20°C, or a mixing of all three variables. Further work that will help to shed light on the role of every variable (headgroup effect, chain effect, and temperature effect) in the nanomechanics of lipid bilayers is an ongoing experiment in our laboratory. In any case, the role of ion-binding on PE bilayers seems to follow the same tendency observed for PC bilayers. Since cations seem to bind through the oxygen carbonyl of the phosphate, the observed tendency is then not surprising, and especially if we take into account that MD simulations have shown similar results for phospholipid heads other than PC, such as phosphatidylserine (51), and also for a mixture of phospholipids (8).

Natural *E. coli* bilayer

After having studied the effect of ion binding on model lipid bilayers, the final issue is to check it on a natural lipid bilayer. To this end, we have performed the same experiment on an *E. coli* polar lipid extract (nominally 67% phosphatidylethanolamine, 23.2% phosphatidylglycerol, and 9.8% cardiolipin). In principle, and according to the fact that we have separately proved that both PC and PE membranes are punctured at a higher force as the ionic strength increases, the same result should be expected for this natural membrane extract. Fig. 13, *a–d*, shows the histograms corresponding to the yield threshold values found for *E. coli* membrane, where the same trend is observed. Fig. 13 *e* shows a topographic image of the *E. coli* membrane, and in Fig. 13 *f* the yield

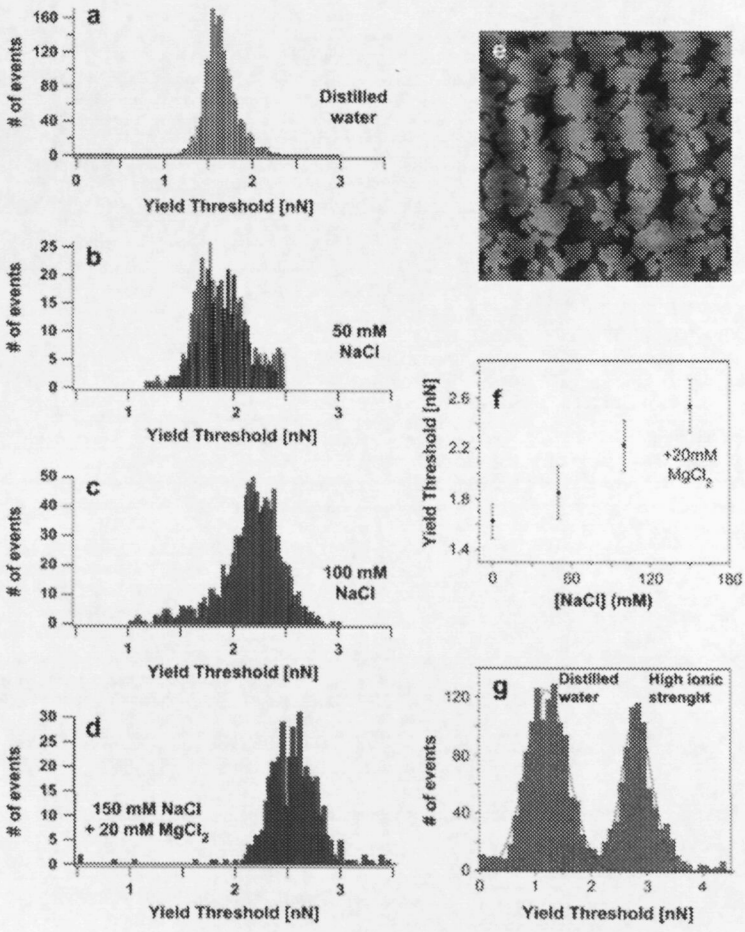

FIGURE 13 (*a–d*) Histograms of the yield threshold force value for *E. coli* bilayers under different ionic compositions: (*a*) 0 mM NaCl, $x = 1.60 \pm 0.14$ nN ($N = 1815$); (*b*) 50 mM NaCl, $x = 1.854 \pm 0.206$ nN ($N = 792$); (*c*) 100 mM NaCl, $x = 2.23 \pm 0.201$ nN ($N = 1252$); and (*d*) 150 mM NaCl + 20 mM $MgCl_2$, $x = 2.54 \pm 0.21$ nN ($N = 591$). All results correspond to a Gaussian fitting of the histograms. (*e*) Contact mode image (5×5 μm^2) of an *E. coli* bilayer deposited on mica. (*f*) Yield threshold values versus ionic strength for the data obtained in histograms *a–d*. Every point stands for the center of the Gaussian fit to the data of the above histograms, whereas error bars represent standard deviations. (*g*) Histograms corresponding to the force plots acquired in distilled water and high ionic strength solution.

threshold force versus ionic strength has been plotted, similar to Fig. 5 for the model membrane. Interestingly, the slope of the plot is ~6 pN/mM, a much lower value than that obtained for the model membrane. Similar results have been obtained for a natural lecithin plant membrane (S. Garcia-Manyes, G. Oncins, and F. Sanz, unpublished). This lower contribution of the added ions on the overall nanomechanical behavior of the system could be interpreted in terms of the complexity of the chemical composition of the system (different phospholipids) that would give rise to a lower packing of the system. However, although this effect is not as outstanding as it was for DMPC, the trend is clearly seen if we compare the histograms for distilled water ($x = 1.60 \pm 0.14$ nN) with those obtained with high ionic strength ($x = 2.54 \pm 0.21$ nN) (Fig. 13 *g*). Histograms for intermediate ionic strengths lie in between, corresponding to the ionic strength concentrations shown in Fig. 13, *b* and *c*.

CONCLUSIONS

We report on a detailed experimental quantitative force spectroscopy study on how ion binding affects model PC lipid membrane nanomechanics. We have experimentally proved that the higher the ionic strength, the higher the force that must be applied with the AFM tip to penetrate the bilayer. These results are in agreement with recent works that have demonstrated both experimentally and theoretically that cations (both monovalent, e.g., Na^+, and divalent, e.g., Ca^{2+}) penetrate the headgroups of phospholipid molecules, giving rise to a more packed phospholipid network and a higher phospholipid-phospholipid lateral interaction. This increase in lateral interaction between neighboring molecules may be the cause for the extension of the elastic deformation region in the force plots before the plastic region begins (yield threshold force value). An elastic spring model that accounts for lateral

interactions has been proved to fit the experimental deformation data. Moreover, we have extended this work to a natural lipid bilayer (*E coli* lipid extract), and the same tendency was observed for the force needed to puncture the bilayer to increase with ionic strength. We provide proof that the binding process is fully reversible and we can estimate directly the kinetics of the membrane response through force spectroscopy measurements. In addition, preliminary results concerning the relationship between nanomechanical response and chemical composition of the hydrophobic tail have been shown. This work introduces a new investigation line dealing with the relationship between the experimental measurements regarding the nanomechanics of membranes in the nanometer/nanonewton range and the atomic underlying processes. This is an interesting example of how small variations in chemical composition both in chemical structure and in the surrounding media can translate into considerable variations in the nanomechanical response of the membrane system.

The authors thank the Departament d'Universitats, Recerca i Societat de la Informacio (Generalitat de Catalunya) for a grant (S.G.M.) and for financial support through projects 2000SGR017 and AGP99 10. We thank Dr. Pau Gorostiza for helpful discussions, Dr. S. Vinzelberg (Asylum Research) for software development, and Dr. T. Missana, Centro de Investigaciones Energeticas Medioambientales y Tecnologicas (Madrid) for kindly allowing us to use the Zetamaster equipment.

REFERENCES

1. Cevc, G. 1990. Membrane electrostatics. *Biochim. Biophys. Acta.* 1031:311–382.
2. Binder, H., and O. Zschornig. 2002. The effect of metal cations on the phase behavior and hydration characteristics of phospholipid membranes. *Chem. Phys. Lipids.* 115:39–61.
3. Ohki, S., N. Duzgunes, and K. Leonards. 1982. Phospholipid vesicle aggregation: effect of monovalent and divalent ions. *Biochemistry.* 21:2127–2133.
4. Ohki, S., S. Roy, H. Ohshima, and K. Leonards. 1984. Monovalent cation induced phospholipid vesicle aggregation: effect of ion binding. *Biochemistry.* 23:6126–6132.
5. Eisenberg, M., T. Gresalfi, T. Riccio, and S. McLaughlin. 1979. Adsorption of monovalent cations to bilayer membranes containing negative phospholipids. *Biochemistry.* 18:5213–5223.
6. Makino, K., T. Yamada, M. Kimura, T. Oka, H. Ohshima, and T. Kondo. 1991. Temperature- and ionic strength-induced conformational changes in the lipid head group region of liposomes as suggested by zeta potential data. *Biophys. Chem.* 41:175–183.
7. Pandit, S. A., D. Bostick, and M. L. Berkowitz. 2003. Molecular dynamics simulation of a dipalmitoylphosphatidylcholine bilayer with NaCl. *Biophys. J.* 84:3743–3750.
8. Pandit, S. A., D. Bostick, and M. L. Berkowitz. 2003. Mixed bilayer containing dipalmitoylphosphatidylcholine and dipalmitoylphosphatidylserine: lipid complexation, ion binding, and electrostatics. *Biophys. J.* 85:3120–3131.
9. Bockmann, R. A., A. Hac, T. Heimburg, and H. Grubmuller. 2003. Effect of sodium chloride on a lipid bilayer. *Biophys. J.* 85:1647–1655.
10. Leonenko, Z. V., A. Carnini, and D. T. Cramb. 2000. Supported planar bilayer formation by vesicle fusion: the interaction of phospholipid vesicles with surfaces and the effect of gramicidin on bilayer properties using atomic force microscopy. *Biochim. Biophys. Acta.* 1509:131–147.
11. Benz, M., T. Gutsmann, N. Chen, R. Tadmor, and J. Israelachvili. 2004. Correlation of AFM and SFA measurements concerning the stability of supported lipid bilayers. *Biophys. J.* 86:870–879.
12. Mueller, H. H. J. Butt, and E. Bamberg. 2000. Adsorption of membrane associated proteins to lipid bilayers studied with an atomic force microscope: myelin basic protein and cytochrome c. *J. Phys. Chem. B.* 104:4552–4559.
13. Desmeules, P., M. Grandbois, V. A. Bondarenko, A. Yamazaki, and C. Salesse. 2002. Measurement of membrane binding between recoverin, a calcium myristoyl switch protein, and lipid bilayers by AFM based force spectroscopy. *Biophys. J.* 82:3343–3350.
14. Kaasgaard, T., C. Leidy, J. H. Ipsen, O. G. Mouritsen, and K. Jorgensen. 2001. In situ atomic force microscope imaging of supported lipid bilayers. *Single Molecules.* 2:105–108.
15. Slade, A. J. Luh, S. Ho, and C. M. Yip. 2002. Single molecule imaging of supported planar lipid bilayer reconstituted human insulin receptors by in situ scanning probe microscopy. *J. Struct. Biol.* 137:283–291.
16. Schneider, J., W. Barger, and G. U. Lee. 2003. Nanometer scale surface properties of supported lipid bilayers measured with hydrophobic and hydrophilic atomic force microscope probes. *Langmuir.* 19:1899–1907.
17. Seantier, B., C. Breffa, O. Felix, and G. Decher. 2004. In situ investigations of the formation of mixed supported lipid bilayers close to the phase transition temperature. *Nano Lett.* 4:5–10.
18. Corcoran, S. G., R. J. Colton, E. T. Lilleodden, and W. W. Gerberich. 1997. Anomalous plastic deformation at surfaces: nanoindentation of gold single crystals. *Phys. Rev. B.* 55:16057–16060.
19. Fraxedas, J., S. Garcia-Manyes, P. Gorostiza, and F. Sanz. 2002. Nanoindentation: toward the sensing of atomic interactions. *Proc. Natl. Acad. Sci. USA.* 99:5228–5232.
20. Ikai, A., and R. Afrin. 2003. Toward mechanical manipulations of cell membranes and membrane proteins using an atomic force microscope: an invited review. *Cell Biochem. Biophys.* 39:257–277.
21. Franz, V., and H. J. Butt. 2002. Confined liquids: solvation forces in liquid alcohols between solid surfaces. *J. Phys. Chem. B.* 106:1703–1708.
22. O'Shea, S. J., and M. E. Welland. 1998. Atomic force microscopy at solid-liquid interfaces. *Langmuir.* 14:4186–4197.
23. Vezenov, D. V., A. Noy, L. F. Rozsnyai, and C. M. Lieber. 1997. Force titrations and ionization state sensitive imaging of functional groups in aqueous solutions by chemical force microscopy. *J. Am. Chem. Soc.* 119:2006–2015.
24. Ahimou, F., F. A. Denis, A. Touhami, and Y. F. Dufrene. 2002. Probing microbial cell surface charges by atomic force microscopy. *Langmuir.* 18:9937–9941.
25. Rief, M., M. Gautel, F. Oesterhelt, J. M. Fernandez, and H. E. Gaub. 1997. Reversible unfolding of individual titin immunoglobulin domains by AFM. *Science.* 276:1109–1112.
26. Schlierf, M., H. Li, and J. M. Fernandez. 2004. The unfolding kinetics of ubiquitin captured with single-molecule force-clamp techniques. *Proc. Natl. Acad. Sci. USA.* 101:7299–7304.
27. Dufrene, Y. F., T. Boland, J. W. Schneider, W. R. Barger, and G. U. Lee. 1998. Characterization of the physical properties of model biomembranes at the nanometer scale with the atomic force microscope. *Faraday Discuss.* 111:79–94.
28. Richter, R. P., and A. Brisson. 2003. Characterization of lipid bilayers and protein assemblies supported on rough surfaces by atomic force microscopy. *Langmuir.* 19:1632–1640.
29. Franz, V., S. Loi, H. Muller, E. Bamberg, and H. H. Butt. 2002. Tip penetration through lipid bilayers in atomic force microscopy. *Colloids Surf. B Biointerfaces.* 23:191–200.
30. Leonenko, Z. V., E. Finot, H. Ma, T. E. Dahms, and D. T. Cramb. 2004. Investigation of temperature-induced phase transitions in DOPC and DPPC phospholipid bilayers using temperature-controlled scanning force microscopy. *Biophys. J.* 86:3783–3793.

31 Lee S, G Sun, V Franz, and H J Butt 2002 Rupture of molecular thin films observed in atomic force microscopy II Experiment *Phys Rev E* 66 031602/1–031602/7

32 Butt, H J, and V Franz 2002 Rupture of molecular thin films observed in atomic force microscopy I Theory *Phys Rev E* 66 031601/1–031601/9

33 Thompson J B, J H Kindt, B Drake, H G Hansma, D E Morse, and P K Hansma 2001 Bone indentation recovery time correlates with bond reforming time *Nature* 414 773–776

34 Ratanabanangkoon P, and A P Gast 2003 Effect of ionic strength on two dimensional streptavidin crystallization *Langmuir* 19 1794–1801

35 Bockmann R A and H Grubmuller 2004 Multistep binding of divalent cations to phospholipid bilayers a molecular dynamics study *Angew Chem Int Ed Engl* 43 1021–1024

36 Newman, M J, and T H Wilson 1980 Solubilization and reconstitution of the lactose transport system from Escherichia coli *J Biol Chem* 255 10583–10586

37 Florin, E L, M Rief, H Lehmann, M Ludwig, C Dornmair, V T Moy, and H E Gaub 1995 Sensing specific molecular interactions with the atomic force microscope *Biosens Bioelectron* 10 895–901

38 Proksch R, T E Schaffer J P Cleveland, R C Callahan and M B Viani 2004 Finite optical spot size and position corrections in thermal spring constant calibration *Nanotechnology* 15 1344–1350

39 Yang J, and J Appleyard 2000 The main phase transition of mica supported phosphatidylcholine membranes *J Phys Chem B* 104 8097–8100

40 Egawa, H, and K Furusawa 1999 Liposome adhesion on mica surface studied by atomic force microscopy *Langmuir* 15 1660–1666

41 Sihn V I, H Wieder, J T Woodward, G Valincius, A Offenhausser, and A L Plant 2002 The role of surface free energy on the formation of hybrid bilayer membranes *J Am Chem Soc* 124 14676–14683

42 Pera, I, R Stark, M Kappl, H J Butt, and F Benfenati 2004 Using the atomic force microscope to study the interaction between two solid supported lipid bilayers and the influence of synapsin I *Biophys J* 87 2446–2455

43 Butt H J 1991 Electrostatic interaction in atomic force microscopy *Biophys J* 60 777–785

44 Pasenkiewicz Gierula, M, Y Takaoka H Miyagawa, K Kitamura and A Kusumi 1997 Hydrogen bonding of water to phosphatidyl choline in the membrane as studied by a molecular dynamics simulation location geometry, and lipid lipid bridging via hydrogen-bonded water *J Phys Chem* 4 101 3677–3691

45 Pasenkiewicz Gierula, M Y Takaoka, H Miyagawa, K Kitamura, and A Kusumi 1999 Charge pairing of headgroups in phosphatidyl choline membranes a molecular dynamics simulation study *Biophys J* 76 1228–1240

46 Israelachvili J 1991 Intermolecular and Surface Forces Academic Press, London

47 Marra J and J Israelachvili 1985 Direct measurements of forces between phosphatidylcholine and phosphatidylethanolamine bilayers in aqueous electrolyte solutions *Biochemistry* 24 4608–4618

48 Tristram-Nagle, S, Y Liu, J Legleiter and J F Nagle 2002 Structure of gel phase DMPC determined by x ray diffraction *Biophys J* 83 3324–3335

49 Ho, C, and C D Stubbs 1997 Effect of n-alkanols on lipid bilayer hydration *Biochemistry* 36 10630–10637

50 Johnson K L 1985 Contact Mechanics Cambridge University Press, Cambridge, UK

51 Pandit, S A, and M L Berkowitz 2002 Molecular dynamics simulation of dipalmitoylphosphatidylserine bilayer with Na+ counter ions *Biophys J* 82 1818–1827

5.4.2 Effect of pH and Ionic Strength on Phospholipid Nanomechanics and on Deposition Process onto Hydrophilic Surfaces measured by AFM

S. Garcia-Manyes, G. Oncins, F. Sanz

Department of Physical Chemistry, Universitat de Barcelona, Spain

Electrochimica Acta 51(24), (2006), 5029-5036

5.4.2.1 Summary

In this work, we explore the effect of the pH and the substrate on the quality of the deposited phospholipid SPBs. Concerning the pH issue, we must remember the SPB formation process: the phospholipid liposomes that are in solution contact the substrate and if they interact favorably with it, the spherical liposome collapses in favor of a planar bilayer. As you may expect, the electrostatic charge of the liposomes and the substrate are extremely important in this deposition process. According to this, the results can be summarized as follows:

- *Zeta potential measurements reveal that the surface charge of PC liposomes is highly dependent on the solution pH and I value. Considering that mica has a residual negative charge, AFM topographic measurements reveal that PC SPBs improve their quality when the liposomes are positively charged. In the case of negative liposomes, the deposition does not take place.*

- *The P_d value in the bilayer breakthrough process decreases as I value increases, suggesting that the presence of ions in the medium modifies the monolayer thickness.*

- *Similar F_y values were obtained for SPBs supported on different substrates (mica, SiO_2 and functionalized mica), suggesting that the substrate morphology does not play a key role on the quality of the bilayer and that the presence of ions is the key factor.*

Available online at www.sciencedirect.com
SCIENCE DIRECT®
Electrochimica Acta 51 (2006) 5029–5036
ELECTROCHIMICA Acta
www.elsevier.com/locate/electacta

Effect of pH and ionic strength on phospholipid nanomechanics and on deposition process onto hydrophilic surfaces measured by AFM

Sergi Garcia-Manyes, Gerard Oncins, Fausto Sanz*

Departament de Physical Chemistry, University of Barcelona, Martí i Franquès 1-11, 08028 Barcelona, Spain

Received 31 May 2005
Available online 19 May 2006

Abstract

The effect of ion binding on a zwitterionic phospholipid such as 1,2 dimyristoyl-sn-glycero 3-phosphocholine (DMPC) has been studied by measuring the zeta potential value of the unilamellar liposomes present in solution while varying the pH and the ionic strength in independent experiments. We have experimentally confirmed that DMPC binds cations resulting in an increase of the zeta potential value. The liposome surface charge has been proved to have a strong effect on the supported bilayer formation on hydrophilic negatively charged surfaces such as mica and silicon oxide as atomic force microscopy images reveal. Furthermore, thanks to force spectroscopy measurements we have proved that ion binding also affects the nanomechanical response of the system, since it increases the force that has to be exerted on the membrane in order to puncture it. Last but not least, the nanomechanics of the bilayer does not depend on the substrate, thus implying that membrane properties are not influenced by the supporting material.
© 2006 Published by Elsevier Ltd

Keywords: Nanomechanics; Biomembranes; AFM; Lipid bilayers; Force Spectroscopy

1. Introduction

Lipid bilayers are the major constituents of cell membrane. Cell membrane separates the extra- from the intracellular matrix, thus playing an important structural role. Furthermore, it provides a barrier that divides electrolytic solutions into different compartments. Therefore, the effect of electrolytic solutions on membranes is of great importance and has deserved wide research [1]. From an experimental point of view, many works have dealt with the quantification of membrane surface potential through the electrophoretic mobility of lipid membranes under solutions with different ionic strength allowing the calculation of the ζ-potential value [2,3]. In a more generic step, the study of the physicochemical properties of lipid bilayers is crucial to understand many biophysical processes that occur at the cell membrane interface [4]. Most of the studies concerning lipid bilayers have been carried out in solution involving their liposome form. In the vicinity of a substrate, these liposomes break and adhere to the substrate, thus forming a continuous bilayer that remains assembled thanks to the high intermolecular forces that bind two neighboring phospholipid molecules together and also to the forces arising between the vesicle and the substrate [5,6]. Such bilayers are known as supported planar bilayers (SPBs), and are found to correctly mimic cell membranes up to an extent [7]. SPBs have been used as model membranes to study cell–cell recognition in the immune system, adhesion of cells, phospholipid diffusion, protein binding to lipid ligands and membrane insertion of proteins [8,9]. Moreover, they have been widely used in biosensor applications [10–15]. Understanding how supported planar lipid bilayers (SPBs) assemble and which are the interaction forces that act between vesicle and substrate surfaces and also between membrane surfaces is fundamental to efforts in chemistry, structural biology, and biophysics [6,16].

Atomic force microscopy (AFM) has revealed to be a powerful tool when it comes to investigating the topographic characteristics of surfaces with subnanometric resolution [17–20]. Concerning SPBs, AFM imaging under liquid environment has provided valuable information regarding SPB spreading, domain separation, topographic evolution with time etc. Besides, thanks to the Force Spectroscopy mode, the measurement of the interaction forces arising between the AFM tip and the studied surface

* Corresponding author. Tel.: +34 93 4021240; fax: +34 93 4021231.
E-mail addresses: sergi.garcia.manyes@ub.es (S. Garcia-Manyes), fsanz@ub.edu (F. Sanz).

0013-4686/$ – see front matter © 2006 Published by Elsevier Ltd.
doi:10.1016/j.electacta.2006.03.062

has been possible. In the particular case of SPB, Force Spectroscopy has allowed to acquire basic information regarding DLVO, hydration and steric forces arisen between lipid bilayers with piconewton resolution [21]. Moreover, the nanomechanics of the system has been also assessed thanks to force spectroscopy measurements. Indeed, the force needed to puncture the membrane has been related to the lateral interaction force arising between two neighboring molecules and can be regarded as a fingerprint of membrane stability. The force needed to puncture the membrane has been reported to depend on the tip approaching velocity [22,23], on the chemical composition of the system [19,21] on the thermodynamic phase of the lipid (temperature) [23,24] and on the ionic strength of the system [25].

Regarding the latter, we have recently proved that the higher the ionic strength, the higher the force needed to penetrate the bilayer with the AFM tip [25]. Indeed, the effect of ion-binding has been proved to largely change some physicochemical properties of the membrane such as the phase transition temperature [26] or the membrane surface potential [2,27,28]. Divalent cations have been shown to effectively bond to the membrane, thus increasing the surface potential value, whereas the role of monovalent cations upon membrane binding has been so far underestimated [29]. Thanks to recent molecular dynamics (MD) simulations [30–32] an atomistic vision of the system has been possible and the obtained results highlight the role of both monovalent and divalent cations upon phospholipid headgroup binding.

There is a three-fold goal in the present paper. On the one hand, we aim to relate the ξ potential evolution of the liposomes with the degree of coverage of an hydrophilic flat surface such as mica (i) as the pH value of the medium is varied and (ii) as the ionic strength of the system is varied. On the other hand, we want to extend these results to another technological important surface such as silicon(1 1 1) + SiO_2. Last but not least, we aim to study whether the nanomechanics of the system depends on the substrate or if, on the contrary, the mechanical response of the membrane is decoupled from the supporting surface. To this purpose, we have studied the nanomechanical properties of the membrane when supported on hydrophilic surfaces such as mica, SiO_2 or freshly annealed gold and also on a hydrophobic surface such as APTES-functionalized mica surface. This information is crucial when studying, e.g. the interaction between supported lipid bilayers and target proteins in possible biosensors applications.

2. Materials and methods

2.1. Sample preparation

1,2-Dimyristoyl-*sn* glycero-3 phosphocholine (DMPC, Sigma, >98%) was dissolved in chloroform/ethanol (3:1) (Carlo Erba, analysis grade, at 99.9%) to give a final DMPC concentration of 2 mM. This dissolution was kept at −10 °C. A 500 μl aliquote was poured in a glass vial and the solvent was evaporated with a nitrogen flow, obtaining a DMPC film at the bottom of the vial. Solution was kept in vacuum overnight to ensure the absence of organic solvent traces. Then, for the experiments performed at different ionic strengths, aqueous solution at the correct ionic strength was added until a final 500 μM DMPC concentration and 0 mM NaCl, 50 mM NaCl, 75 mM NaCl, 100 mM NaCl and 150 mM NaCl + 20 mM $MgCl_2$ respectively and pH was set to 7.4 with 10 mM Hepes/NaOH. In the case of the experiments performed at different pH, several buffer solutions were used, pH 4 was attained with HAc, pH 7 with HEPES, pH 10 with Tris and pH 2 and 12 were attained with HCl and NaOH, respectively. In order to maintain a constant ionic strength, buffer concentration was set to 10 mM for all samples. Because of the low solubility of DMPC in water, the vial was subjected to 30 s cycles of vortexing, temperature and sonication until the obtention of a homogeneous mixture. The solution was finally sonicated for 20 min (in order to have unilamellar liposomes) and let it settle overnight always protected from light and maintained at 4 °C. Prior to its use, mica surfaces (Metafix, CLLS grade) were glued onto Teflon discs with a water insoluble mounting wax. A 50 μl of DMPC dissolution at the specific NaCl concentration were applied to cover 0.5 cm^2 freshly cleaved pieces of mica for a deposition time of 35 min. After that, mica was rinsed three times with 100 μl of the corresponding ionic aqueous solution. The same procedure was followed when the substrate used was silicon oxide (silicon(1 1 1) wafers, Siltronix (Archamps, France)) *n* phosphor, 5–15 Ω cm, thickness 500–550 μm have been etched with hydrofluoric acid (Merck, Suprapur, Germany) and native oxide was let grow for four days under controlled atmosphere.

The gold substrate was provided by Arrandee (Werther, Germany). Briefly, it consists of a borosilicate glass covered with a chromium layer 1–4 nm thick on the top of which a gold layer 200–300 nm thick is deposited. This surface is immersed in piranha solution for 10 min, extensively rinsed with ethanol and dried with a nitrogen flow. Then, the gold surface is flame annealed (butane flame) for 3 min and cooled under nitrogen. This process results in a clean, hydrophilic gold surface [33].

Hydrophobic amine-functionalized mica surfaces were prepared by simply exposing freshly cleaved mica to (3-aminopropyl)dimethoxysilane (APTES, Aldrich) vapours under low pressure conditions for 30 s [34].

2.2. Zeta potential measurements

ξ-Potential measurements were performed with a Zetamaster Particle Electrophoresis Analyser through which the velocity of the particles can be measured with a light scattering technique by using the Doppler effect thanks to a pair of mutually coherent laser beams (5 mW, He–Ne laser at 633 nm). Zetamaster measures the autocorrelation function of the scattered light and after the signal processing it obtains the electrophoretic mobility and, finally, through the Henry equation, the ξ-potential.

2.3. AFM imaging

AFM images were acquired with a Dimension 3100 (Digital Instruments, Santa Barbara) microscope controlled by a Nanoscope IV electronics (Digital Instruments, California) in

contact mode using V-shaped Si_3N_4 tips (OMCL TR400PSA, Olympus, Japan) cantilevers. The applied force was controlled by acquiring force plots before and after every image was captured.

2.4. Force spectroscopy

Force spectroscopy was performed with a Molecular Force Probe1-D (MFP), Asylum Research (Santa Barbara, CA). Force plots were acquired using V-shaped Si_3N_4 tips (OMCL TR400PSA, Olympus, Japan) with a nominal spring constant of 0.08 N/m. Individual spring constants were calibrated using the equipartition theorem (thermal noise) [35] after having correctly measured the optical lever sensitivity (V/nm) by measuring it at high voltages after several minutes of performing force plots to avoid hysteresis. It has to be pointed out that the results here shown for DMPC bilayers were obtained with the same cantilever keeping the spot laser at the same position on the lever to avoid changes in the spring constant calculation [36]. However, results have low scattering when using different tips and different samples. About 1300 curves over more than 15 positions were obtained for each sample. All force spectroscopy and AFM images were obtained at 20 ± 0.5 °C, which is below the main phase transition temperature (T_m) of DMPC (23.5 °C). Besides, we have to consider here that T_m for supported bilayers shifts to a higher temperature than observed in solution [37]. Therefore, we are indenting the gel phase for DMPC supported bilayers. Applied forces F are given by $F = k_c \Delta$ where is the cantilever deflection. The surface deformation is given as penetration (δ) evaluated as $\delta = z - \Delta$, where z represents the piezo-scanner displacement.

3. Results and discussion

3.1. The role of pH and ionic strength upon vesicle fusion and deposition

In the process of vesicle fusion into a flat bilayer, surface energy seems to play an important role [38]. Freshly cleaved mica is negatively charged under a wide range of ionic strength and pH [39]. Fig. 1a shows the evolution of the ξ-potential value while varying the pH value of the measuring solution by maintaining a constant ionic strength, which corresponds to an electroanalytical titration of the lipid bilayer [40]. At a first sight, an increase of the ξ-potential value as the pH value decreases is observed. This experimental observation indicates that H^+ are bond to the choline moiety of the phospholipid headgroup, in particular to the phosphate group of the phosphatidylcholine moiety, since it is the only chemical group that holds ionizable groups. Interestingly, even though phosphatidylcholine is a zwitterionic headgroup, it exhibits a net negative charge at neutral pH. This has been interpreted in terms of hydration layers formed around the surface [39] and to the orientation of lipid headgroups [3]. It is important to point out that the ξ-potential measurements do not yield direct information of the surface charge, but of the charge measured at the point where the Stern layer and the diffuse layer meet (shear plane). However, it is considered to yield a significant approximation of the surface potential. The titration of phosphatidylcholine lipid bilayers with chemically functionalized AFM tips has been experimentally addressed elsewhere [41]. According to Fig. 1a, DMPC liposomes exhibit negative charge at pH > ~3.5 and positive charge at pH < ~3.5. At pH 3.5–4 the zero charge potential is found. According to those

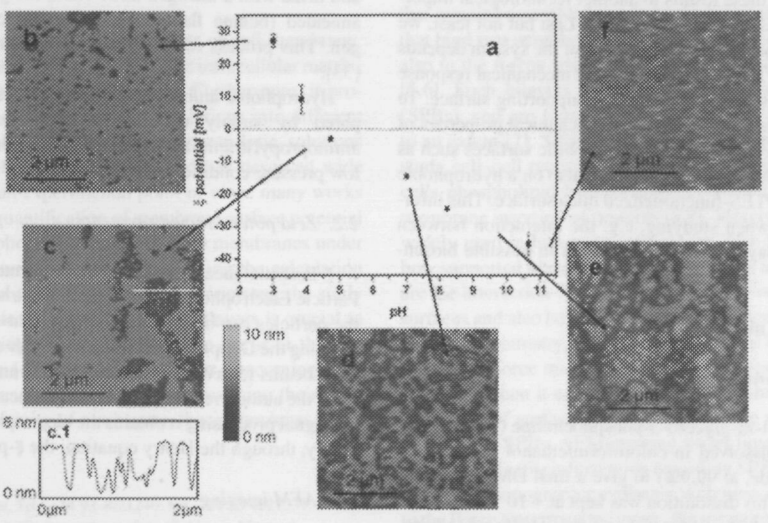

Fig. 1. (a) Evolution of the ξ-potential value of a DMPC unilamellar liposome solution as the pH value is varied. The ionic strength of each measuring solution is kept constant at 10 mM. A 5 μm × 5 μm contact mode AFM images of a mica-supported DMPC bilayer formed and deposited at different pH values: (b) 2, (c) 4, (d) 7, (e) 10 and (f) 12. Note that images do not correspond exactly to the pH values at which the ξ-potential has been measured in (a). (c.1) A cross-section profile of the bilayer in order to measure the bilayer height.

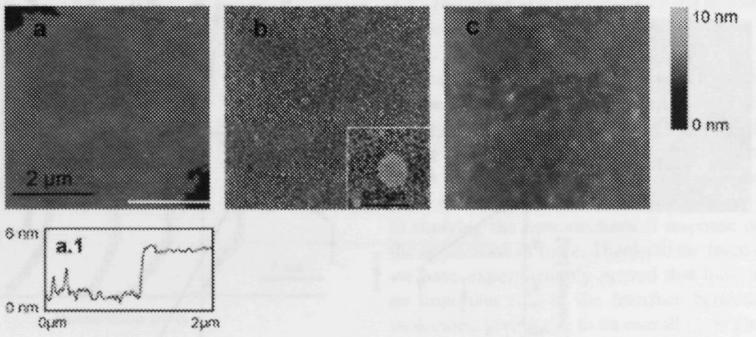

Fig. 2. A 5 μm × 5 μm contact mode AFM images of a SiO_2-supported DMPC bilayer formed and deposited at different pH values: (a) 2, (b) 7 and (c) 12. (a.1) A cross-section profile of the bilayer in order to measure the bilayer height.

results, and taking into account that mica is negatively charged, a high degree of surface coverage should be expected at pH < 4 and a lower degree of surface coverage should be expected at higher pH values if the global vesicle fusion process is assumed to be electrostatically governed. Fig. 1b shows a 5 μm × 5 μm AFM contact mode image corresponding to a DMPC bilayer formed and deposited at pH 2. The mica surface is practically fully covered at this pH value (87% surface coverage). The surface coverage ratios shown correspond with the mean value of the analysis of at least five images obtained on each sample at different locations. The darker holes correspond to the mica surface and can be used to assess the height of the bilayer, 4.6 ± 0.3 nm. Fig. 1c shows a 5 μm × 5 μm AFM contact mode image where the DMPC bilayer has been formed and deposited at pH 4. In this case, a compact huge bilayer is also observed, even though in this case the uncovered mica surface region is higher than in Fig. 1b (74% surface coverage). A cross-section of Fig. 1c is shown in Fig. 1c.1, where the height of the bilayer can be measured to be 4.5 ± 0.3 nm. Fig. 1d–f also shows 5 μm × 5 μm images of a DMPC bilayer formed and deposited at pH 7.0 (Fig. 1d), pH 10 (Fig. 1e) and pH 12 (Fig. 1f). It is clear that as the pH value is increased and the surface potential acquires a more negative value, the degree of bilayer coverage decreases (55% at pH 7.0, 48% at pH 10 and 32% at pH 12), and the formed bilayers are less compact and far less fusioned. We conclude, then, that pH has an important effect on membrane deposition on mica. In order to check whether this tendency is also observed with other hydrophilic substrates, we have performed the same deposition procedure on a Si(1 1 1) substrate exhibiting a native SiO_2 layer on its surface. Silicon oxide surface exhibits negative charge at pH values >3.5 and almost no charge (fully protonated species) at lower pH values [42]. Fig. 2 shows 5 μm × 5 μm AFM contact mode images of a DMPC bilayer formed and deposited at pH 2 (Fig. 2a), pH 7 (Fig. 2b) and pH 12 (Fig. 2c). These results indicate that the same tendency observed upon mica deposition is observed on SiO_2 surface: at low pH values (liposome positively charged), the deposition and spreading of the bilayer on the negatively charged surface is favored (Fig. 2a, 89% surface coverage) whereas at higher pH values (Fig. 2b), electrostatic repulsion between negatively charged liposome and surface results in a low degree of surface coverage or even in an absence of surface coating (Fig. 2c, 5–8% surface coverage). The cross-section profile of Fig. 2a (Fig. 2a.1) allows to measure the height of the supported bilayer (4.7 ± 0.2 nm), which is in very good accordance with the obtained results observed in Fig. 1c.1.

In order to systematically study the role of ionic strength on the liposome fusion process we have reproduced the same experiment depicted in Fig. 1. In this case, we have kept constant the pH value (pH 7) and we have measured the zeta potential value at different ionic strengths. The results are shown in Fig. 3a. According to these results, at pH 7 liposomes are negatively charged from 0 mM ionic strength (deionized water pH 7, −12 ± 1.6 mV) to 100 mM NaCl, where the zero charge point is found. Upon further increasing the ionic strength value up to physiological values (150 mM NaCl + 20 mM $MgCl_2$) a net positive zeta potential is measured (6.86 ± 2.3 mV), resulting in a positive surface charge. The probable divalent cation preference for membrane binding [43] may also help to reverse the obtained net zeta potential value (from negative values to positive values). Recalling the negative surface charge of mica at different ionic strengths, the process of vesicle deposition and fusion into a flat bilayer may be also favored at high ionic strengths (negative surface-positive liposome surface) in view of the electrokinetic results observed in Fig. 3a. This is experimentally confirmed upon AFM contact mode images. Fig. 3b–e shows a 5 μm × 5 μm images of a DMPC bilayer formed and deposited at 0 mM NaCl (Fig. 3b), 50 mM NaCl (Fig. 3c), 100 mM NaCl (Fig. 3d) and 150 mM NaCl + 20 mM $MgCl_2$ (Fig. 3e). As it can be clearly observed, as the ionic strength of the system increases, the degree of surface coverage is also increased (51% at 0 mM NaCl, 68% at 50 mM NaCl, 80% at 100 mM NaCl and 91% at 150 mM NaCl + 20 mM $MgCl_2$) since the zeta potential value becomes less negative (or even positive at high ionic strength).

3.2. The role of ionic strength on the nanomechanics of DMPC bilayers

So far we have dealt with the role of ion binding and pH on the deposition process of unilamellar liposomes onto

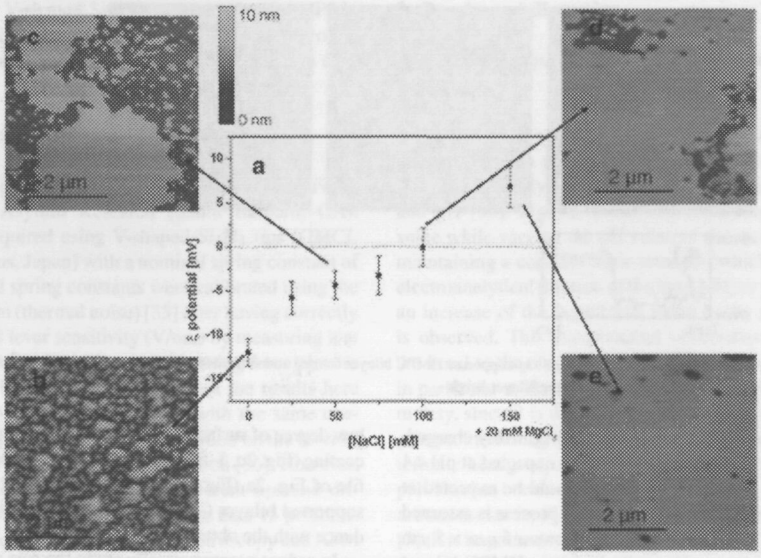

Fig. 3. (a) Evolution of the ξ-potential value of a DMPC unilamellar liposome solution as the ionic strength of the measuring solution is varied. The pH value of each measuring solution is kept constant at pH 7. A 5 μm × 5 μm contact mode AFM images of a mica-supported DMPC bilayer formed and deposited under different ionic strength values: (b) 0 mM NaCl, (c) 50 mM NaCl, (d) 100 mM NaCl and (e) 150 mM NaCl + 20 mM $MgCl_2$.

hydrophilic surfaces, i.e. the role that cations play within the surface–liposome interface. Besides, cations also play an important role upon binding two neighboring phospholipid molecules together through the carbonyl of the headgroup, thus creating a huge network linked through cations and water molecules, as recent molecular dynamics simulations predict. The cation-binding process results then in a closer distance between molecules (lower area per molecule value) yielding a more packed structure, which increases the strength of lateral interactions between neighboring molecules. This molecular reorganization in the presence of cations is related to a different (nano)mechanical response of the membrane upon the application of force. Indeed, the increase of lateral interactions can be assessed thanks to the increase in the force needed to puncture the membrane with the AFM tip as the ionic strength of the system is increased. This fact can be observed in Fig. 4A, where five force curves on a DMPC bilayer are shown. In Fig. 4A(a), the membrane was formed and deposited under deionized water, pH 7.4, and the membrane indentation (which is related to the discontinuity in the plot) occurs at 3.7 nN. This force value corresponds to the force at which the tip penetrates the membrane, which is related to the onset of plastic deformation. In Fig. 4A(b) (50 mM NaCl) the yield threshold occurs at 6.0 nN. Upon increasing the ionic strength up to 75 mM NaCl (Fig. 4A(c)) the yield threshold value occurs at 9.0 nN, at 100 mM NaCl (Fig. 4A(d)) the yield threshold force occurs at 11.1 nN, and finally, at high ionic strength (150 mM NaCl + $MgCl_2$, which mimics physiological conditions) the yield threshold force value occurs at 15.1 nN (Fig. 4A(e)). According to these results it seems clear that the effect of ion-binding is related to the increase of membrane resistance upon breakthrough. These values are statistically confirmed in a recent publication, where we also analyzed the different forces that play a significant role in the nanomechanics of the lipid bilayers [25]. According to these experimental results, DLVO forces occurring between the substrate and the AFM tip only account for the first stages of the force plot (range up to a few hundreds of pN). At higher forces, the membrane deforms elastically until it is no longer able to withstand the force exerted by the AFM tip. At this moment the tip penetrates the membrane giving rise to a discontinuity in the force–distance curve. The width of the jump is related to the height of the membrane, as it is shown in Fig. 4B, where the evolution of the width of the jump with ionic strength is shown. According to these results, the width of the jump decreases with the ionic strength until reaching a plateau at ~75 mM. This trend can be interpreted in terms of the role that the elastic deformation plays upon the membrane nanomechanics: at low ionic strengths the membrane compactness is rather limited and therefore the membrane is easily punctured, and the width of the jump accounts for the total height of the membrane, as assessed through AFM images. At higher ionic strengths, however, the bilayer can be elastically deformed before being penetrated by the AFM tip. During this elastic deformation the AFM tip is exerting an increasingly higher force on the membrane, so that the membrane can be elastically squeezed. When the membrane is no longer able to withstand this applied force, the jump in the force plot occurs, and in this case the distance that the AFM tip has to travel to reach the substrate is lower (less piezo-displacement) since the bilayer had been previously elastically deformed. The force at which the mem-

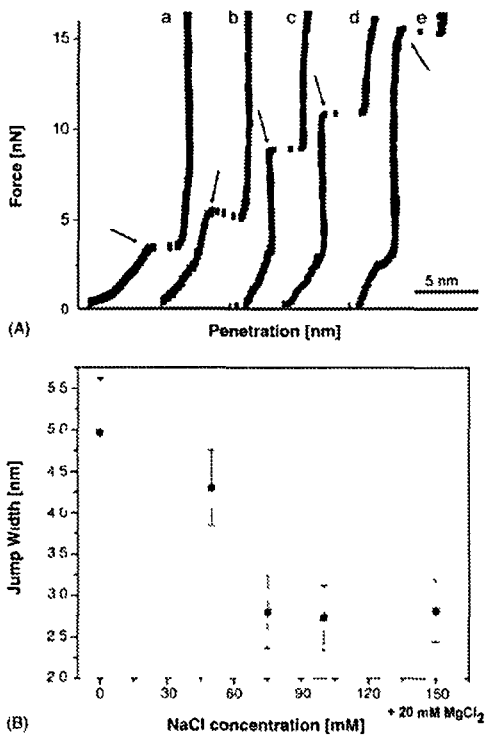

Fig. 4. (A) Force–distance curves obtained on a mica supported DMPC bilayer. For simplicity only the extending curves are shown. The discontinuity in the graph (yield threshold force value, pointed with an arrow) stands for the force value at which the tip penetrates the membrane i.e. the onset of plastic deformation. Every force plot has been acquired at a different ionic strength value: (a) 0 mM NaCl, (b) 50 mM NaCl, (c) 75 mM NaCl, (d) 100 mM NaCl and (e) 150 mM NaCl + 20 mM $MgCl_2$. As it can be seen from the graph the higher the ionic strength the higher the yield threshold force value. (B) Evolution of the jump width with the ionic strength. All results correspond to a Gaussian fitting of the data collected at different ionic strengths: 0 mM NaCl ($z = 1.97 \pm 0.01$ nm ($N = 263$)); 50 mM NaCl ($z = 1.31 \pm 0.03$ nm ($N = 211$)); 75 mM NaCl ($z = 2.80 \pm 0.03$ nm ($N = 290$)); 100 mM NaCl ($z = 2.73 \pm 0.03$ nm ($N = 222$)) and 150 mM NaCl + 20 mM $MgCl_2$ ($z = 2.52 \pm 0.03$ nm ($N = 230$)).

brane breaks (onset of plastic deformation) can be then easily assessed by the discontinuity in the force plot. The force at which this discontinuity occurs can be then regarded as the fingerprint of membrane (nano)mechanical stability and it is related to the tip approaching velocity [22], ionic strength [25], temperature [24] and phospholipid chemical composition of the bilayer [44]. The same tendency has been observed upon lateral force microscopy studies [45]. Therefore, we come to the conclusion that atomic force microscopy through its force spectroscopy mode is the only technique that allows to have a picture of the nanomechanics of the process at the nanonewton scale and at the single molecule level besides molecular dynamics simulations.

3.3. The effect of the substrate on the nanomechanics of the system

Thanks to the use of the atomic force microscopy images we have assessed that liposome fusion and deposition is a process that is highly dependent on the pH and the ionic strength of the measuring medium, two important variables to be kept under control in electrochemistry experiments. Furthermore, force spectroscopy reveals to be the suitable tool when it comes to studying the nanomechanical response of the bilayer under the application of force. Thanks to the force spectroscopy mode we have experimentally proved that ionic strength plays also an important role in the interface between two neighboring molecules, giving rise to an overall more packed structure with enhanced mechanical response. Next step is then to decouple the (possible) contributions of the substrate on the nanomechanical behavior of the membrane. Indeed, in biosensor technology it is important to assess that the properties of the functionalized layer are (little) influenced by the nature of the substrate in order to have reproducible results. To this aim we have compared the nanomechanical response of a DMPC bilayer deposited on mica at 0 mM NaCl (deionized water) pH 7 (Hepes/OH) with the nanomechanical response of the same membrane under the same experimental conditions deposited on the SiO_2 substrate and also under freshly annealed (hydrophilic) [33] gold. The histograms corresponding to the breakthrough forces for the three experiments are shown in Fig. 5. Fig. 5a shows the histogram corresponding to the yield threshold force obtained on a DMPC bilayer supported on mica, whereas the histogram shown in Fig. 5b corresponds to the same bilayer supported on SiO_2 and on gold (Fig. 5c). Gaussian fitting to Fig. 5a yields a threshold force value of 3.11 ± 0.35 nN whereas in the case of Fig. 5b the yield threshold force value occurs at 3.28 ± 0.07 nN and in the case of gold the yield threshold force value occurs at 3.44 ± 0.13 nN. Therefore, the difference between the results concerning the three substrates is ~9%, which is lower than the uncertainty obtained for spring constant calibration (~15%) [46]. We can conclude then, that we are indeed measuring the "true" nanomechanical response of the bilayer and that no effect of the substrate is found upon statistical treatment of the yield threshold force value data. Finally, we have conducted the same experiment on a hydrophobic substrate [34] such as APTES-functionalized mica surface. In this case, the bilayer would probably acquire a reverse structure, with the hydrophobic tails facing the substrate. Therefore, it is interesting to assess whether the reverse conformation of the bilayer would give rise to the same yield threshold force value than the one observed for the three hydrophilic substrates above commented. Fig. 5d shows the histogram corresponding to the yield threshold values of a DMPC bilayer supported in the mica-functionalized substrate. Gaussian fitting to the histogram yields the force value of 3.69 ± 0.12 nN. Although further experiments on different hydrophobic substrates such as graphite should be conducted these preliminary results suggest that the mechanical resistance of the bilayer at the nanometer scale remains the same regardless of the orientation that the bilayer acquires in the deposition process as a consequence of the hydrophilic/hydrophobic nature of

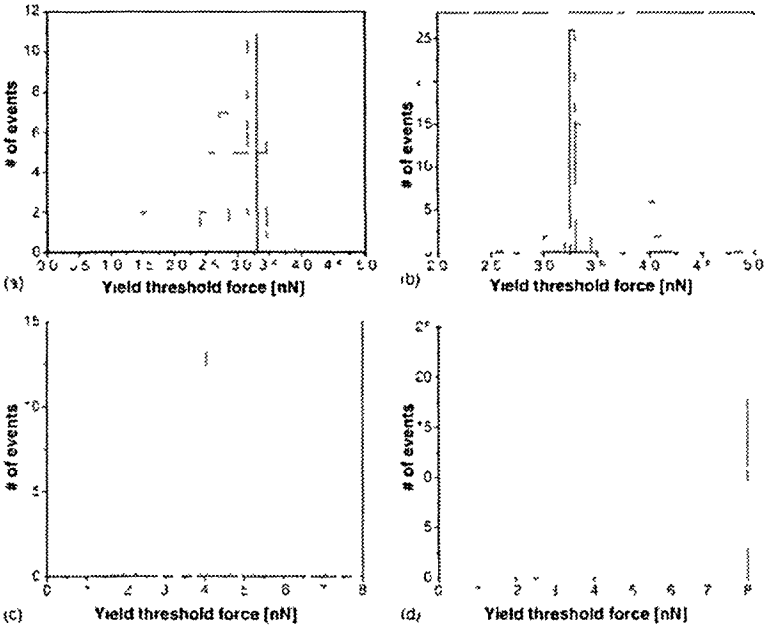

Fig. 5. Histograms corresponding to the yield threshold force value obtained on DMPC bilayers assembled at 0 mM NaCl pH 7. The DMPC bilayer was supported on (a) mica, (b) SiO$_2$, (c) gold and (d) APTES functionalized mica substrates. Gaussian fitting to the histograms yields (a) $x_c = 3.11 \pm 0.35$ nN ($N = 30$), (b) 3.28 ± 0.07 nN ($N = 57$), (c) 3.44 ± 0.13 nN ($N = 75$), and (d) 4.63 ± 0.12 nN ($N = 73$).

the substrate. Nonetheless, in the case of hydrophobic substrates the driving force of the deposition process may most likely be non electrostatic.

4. Conclusions

In this work we have experimentally proved that pH and ionic strength have a great effect on supported planar bilayer deposition and spreading onto hydrophilic substrates such as mica and silicon oxide. This process seems to be electrostatically governed since the degree of surface coverage strongly depends on the liposome surface charge as zeta potential measurements reveal. These measurements allow us to experimentally confirm that zwitterionic lipid bilayers such as phosphatidylcholine actually bind both monovalent and divalent cations in their head group moiety. The effect of ion-binding not only does influence on planar bilayer formation, but it also has a crucial effect on membrane nanomechanics since it increases a great deal the lateral interactions between neighboring molecules with the overall result of an increase of the force required to penetrate the membrane. Force spectroscopy seems to be then the suitable tool to investigate the nanomechanical response of the bilayer at the nanometer scale, thanks to the jump present in the force curve, which fingerprints membrane stability. Thanks to this experimental technique we have experimentally proved that the nanomechanics of the bilayer does not depend on the substrate, thus implying that membrane properties are not influenced by the supporting material, which is important in a view to e.g. biosensors designing.

Acknowledgements

One of the authors (S.G.-M.) thanks Departament d'Universitats i Societat de la Informacio (Generalitat de Catalunya) for a grant and all the financial support through projects 2000SGR017 and AGP99-10.

References

[1] G. Cevc, Biochim. Biophys. Acta 1031 (1990) 311.
[2] M. Eisenberg, T. Gresalfi, T. Riccio, S. McLaughlin, Biochemistry 18 (1979) 5213.
[3] K. Makino, T. Yamada, M. Kimura, T. Oka, H. Ohshima, T. Kondo, Biophys. Chem. 41 (1991) 175.
[4] J.F. Nagle, S. Tristram-Nagle, Biochim. Biophys. Acta Rev. Biomembr. 1469 (2000) 159.
[5] J. Bass, J. Israelachvili, G. Pan, Biophys. J. 79 (2000) 3153.
[6] A.V. Tkachenko, A. Cunnane, D.T. Grandy, Biochim. Biophys. Acta 1509 (1998) 131.
[7] E. Sackmann, Science 271 (1996) 43.
[8] B. Mueller, B.E. Bair, J. Bamberg, J. Phys. Chem. B 104 (2000) 1552.
[9] P. Desmeules, M. Grandbois, V.A. Bendersky, A. Yamazaki, C. Salesse, Biophys. J. 82 (2002) 3343.
[10] D. Ohlenbacher, R. Kinder, ter, P. Gunnet, B. Klee, F. Jahnig, W. Geppert, Sens. Actuators, B, Chem. 1 (1990) 92.
[11] D.P. Nikolelis, C.G. Siontorou, V.G. Andreou, Lab. Robot. Autom. 9 (1997) 255.

[12] D.P. Nikolelis, S.S.E. Petropoulou, E. Pergel, K. Toth, Electroanalysis 14 (2002) 783
[13] D.P. Nikolelis, S.S.F. Petropoulou, G. Theoharis, Electrochim. Acta 47 (2002) 3457
[14] D.P. Nikolelis, S.S.F. Petropoulou, M.V. Mitrokotsa, Bioelectrochemistry 58 (2002) 107
[15] N. Sugao, M. Sugawara, H. Minami, M. Uto, Y. Umezawa, Anal. Chem. 65 (1993) 363
[16] M. Benz, T. Gutsmann, N. Chen, R. Tadmor, J. Israelachvili, Biophys. J. 86 (2004) 870
[17] T. Kaasgaard, C. Leidy, J.H. Ipsen, O.G. Mouritsen, K. Jorgensen, Single Mol. 2 (2001) 105
[18] A. Slade, J. Luh, S. Ho, C.M. Yip, J. Struct. Biol. 137 (2002) 283
[19] J. Schneider, Y.F. Dufrene, W.R. Barger Jr., G.U. Lee, Biophys. J. 79 (2000) 1107
[20] B. Seantier, C. Breffa, O. Felix, G. Decher, Nano Lett. 4 (2004) 5
[21] Y.F. Dufrene, T. Boland, J.W. Schneider, W.R. Barger, G.U. Lee, Faraday Discuss. (1998) 79
[22] S. Loi, G. Sun, V. Franz, H.J. Butt, Phys. Rev. e66 (2002)
[23] V. Franz, S. Loi, H. Muller, T. Bamberg, H.H. Butt, Colloids Surf. B Biointerfaces 23 (2002) 191
[24] S. Garcia-Manyes, G. Oncins, F. Sanz, Biophys. J. 89 (2005) 4261
[25] S. Garcia-Manyes, G. Oncins, F. Sanz, Biophys. J. 89 (2005) 1812
[26] J.M. Sturtevant, Chem. Phys. Lipids 95 (1998) 163
[27] S. Ohki, N. Duzgunes, K. Leonards, Biochemistry 21 (1982) 2127
[28] S. Ohki, S. Roy, H. Ohshima, K. Leonards, Biochemistry 23 (1984) 6126
[29] R.A. Bockmann, A. Hac, T. Heimburg, H. Grubmuller, Biophys. J. 85 (2003) 1647
[30] R.A. Bockmann, H. Grubmuller, Angew. Chem. Int. Ed. Engl. 43 (2004) 1021
[31] S.A. Pandit, D. Bostick, M.L. Berkowitz, Biophys. J. 84 (2003) 3743
[32] S.A. Pandit, M.L. Berkowitz, Biophys. J. 82 (2002) 1818
[33] P. Gupta, A. Ulman, S. Fanfan, A. Korniakov, K. Loos, J. Am. Chem. Soc. 127 (2005) 4
[34] D.V. Vezenov, A. Noy, L.F. Rozsnyai, C.M. Lieber, J. Am. Chem. Soc. 119 (1997) 2006
[35] E.L. Florin, M. Rief, H. Lehmann, M. Ludwig, C. Dornmair, V.T. Moy, H.E. Gaub, Biosens. Bioelectron. 10 (1995) 895
[36] R. Proksch, T.F. Schaffer, J.P. Cleveland, R.C. Callahan, M.B. Viani, Nanotechnology 15 (2004) 1344
[37] J. Yang, J. Appleyard, J. Phys. Chem. B 104 (2000) 8097
[38] V.I. Silin, H. Wieder, J.T. Woodward, G. Valincius, A. Offenhausser, A.L. Plant, J. Am. Chem. Soc. 124 (2002) 14676
[39] H. Egawa, K. Furusawa, Langmuir 15 (1999) 1660
[40] H.C. Tsui, D.M. Ojcius, W.L. Hubbell, Biophys. J. 49 (1986) 459
[41] S. Garcia-Manyes, P. Gorostiza, F. Sanz, Anal. Chem. 78 (2006) 61
[42] S.W. Ong, X.L. Zhao, K.B. Eisenthal, Chem. Phys. Lett. 191 (1992) 327
[43] J. Marra, J. Israelachvili, Biochemistry 24 (1985) 4608
[44] S. Garcia-Manyes, G. Oncins, F. Sanz, Effect of phospholipid chemical composition on the nanomechanics of lipid bilayers by force spectroscopy, in preparation
[45] G. Oncins, S. Garcia-Manyes, F. Sanz, Langmuir 21 (2005) 7373
[46] H.J. Butt, M. Jaschke, Nanotechnology 6 (1995) 1

5.4.3 Study of Frictional Properties of a Phospholipid Bilayer in a Liquid Environment with Lateral Force Microscopy as a Function of NaCl Concentration

G. Oncins, S. Garcia-Manyes, F. Sanz

CREBEC and Department of Physical Chemistry, Chemistry Faculty, University of Barcelona, Martí i Franquès 1-11, 08028, Barcelona Spain

Langmuir 21, (2005), 7373-7379

5.4.3.1 Summary

This work represents the logical step forward after the paper presented in section 5.4.1. The nanomechanics of phospholipid SPBs had been studied by Force Spectroscopy, that is, by applying a vertical compression to the sample, and the samples proved to be more resistant as *I* value increased. Now it was time to study their frictional behavior to complete the nanomechanics characterization of the bilayers. To do that, we developed an LFM system able to work in liquid environment, which was a real challenge, as there was only one previous paper that presented quantitative LFM experiments in liquid medium[331]. The obtained results can be summarized as follows:

- *The F_f vs. F_v curves obtained on PC SPBs in liquid environment revealed the presence of three nanotribological regimes. First of all, an extremely low F_f value region at low loads corresponding with a soft contact between the tip and the sample. The DLVO model predicts an electrostatic repulsion between the two surfaces so the lubricant behavior of the bilayer in this regime is due to the long-distance interaction between them. In simple words, the tip is surfing on the*

surface of the electrochemical double layer, while the bilayer surface remains untouched. The second regime is reached when the tip contacts the sample and deforms it. As a consequence, there is a sharp increment of the F_f value. Finally, the tip contacts the substrate. Interestingly, the range of F_v values corresponding to each regime is heavily affected by the presence of ions in the medium. Basically, the disruption of the bilayer takes place at higher F_v values as I increases, in accordance with previous Force Spectroscopy experiments.

- *The topographic signal recorded simultaneously to the friction measurements reveal that the presence of ions highly modifies the bilayer recovery velocity. Then, bilayers in pure MilliQ water quickly recover from the damage inflicted by the tip during the friction experiment while, in the case of a bilayer in physiological environment, the sample damage remains after the conclusion of the F_f vs. F_v experiment.*

Langmuir **2005**, *21* 7373 7379

Study of Frictional Properties of a Phospholipid Bilayer in a Liquid Environment with Lateral Force Microscopy as a Function of NaCl Concentration

Gerard Oncins, Sergi Garcia-Manyes, and Fausto Sanz

CREBEC and Department of Physical Chemistry, Chemistry Faculty University of Barcelona Martí i Franques 1 11, 08028 Barcelona Spain

Received March 9, 2005 In Final Form May 23 2005

Friction properties of 1 2 dimyristoyl *sn* glycero 3 phosphocholine (DMPC) supported planar bilayers deposited on mica were tested in a liquid environment by lateral force microscopy The presence of these bilayers was detected by imaging and force measurements with atomic force microscopy To test how the presence of NaCl affects the frictional properties of the phospholipid bilayers four DMPC bilayers were prepared on mica in saline media ranging from 0 to 0 1 M NaCl Changes in the lateral vs vertical force curves were recorded as a function of NaCl concentration and related to structural changes induced in the DMPC bilayer by electrolyte ions Three friction regimes were observed as the vertical force exerted by the tip on the bilayer increased To relate the friction response to the structure of the DMPC bilayer topographic images were recorded at the same time as friction data Ions in solution screened charges present in DMPC polar heads leading to more compact bilayers As a consequence the vertical force at which the bilayer broke during friction experiments increased with NaCl concentration In addition the topographic images showed that low NaCl concentration bilayers recover more easily due to the low cohesion between phospholipid molecules

Introduction

Self assembled phospholipid layers have been extensively researched in recent decades The fact that these structures are common in cell membranes has led to their use as models for the study of a wide variety of biological questions such as ion channel imaging in cell membranes,[1] biomembrane modeling and a great many processes in the fields of biophysics, chemistry[2] and medicine Phospholipid layers are particularly important in cancer research[3] and biosensor development[4] Supported planar bilayers (SPBs)[5,6] are widely used to study interaction and adhesion forces between cells and between individual phospholipid molecules, diffusion of phospholipids, and insertion of proteins into membranes[7,8] The nature of these two dimensional layers has permitted the study of electrostatic, steric and van der Waals forces that maintain their cohesion SPBs have been obtained on several kinds of surfaces, such as glass, silicon silicon nitride, quartz, and mica,[9] and with various deposition techniques[10-12] namely, spin coating,[13] Langmuir–Blodgett[11] layer formation liposome deposition,[1] and rupture of natural cell membranes[1] Atomic force microscopy (AFM) has proved a suitable technique for the study of such systems as it sheds light on the structure and topography of SPBs Previously scanning tunneling microscopy (STM) had been used to obtain high resolution images of amphiphilic lipid bilayers[1,18] although the nonconducting nature of the phospholipid bilayers led to some controversy about the interpretation of the images obtained With AFM the molecular topographic resolution of these systems[19-21] and the morphology of SPBs under various conditions could be studied[2,22] In addition to the surface force apparatus (SFA),[8] AFM is a sensitive and versatile technique for testing the mechanical properties of monolayers bilayers, and thin films in an extremely local way, offering a wide substrate choice and range of pressures applied to the layer

(1) Wu Z Tang J Cheng Z Yang X Wang E *Anal Chem* **2000** *72* 6030
(2) Leonenko Z V Carnini A Cramb D T *Biochim Biophys Acta* **2000** *1509* 131
(3) Siontorou C G Andreou V G Nikolelis D P Krull U J *Electroanalysis* **2000** *12* 747
(4) Wu Z Wang B Chang Z Yang X Dong S Wang F *Biosen Bioelectron* **2001** *16* 47
(5) Silvestro L Axelsen P H *Chem Phys* **1998** *96* 69
(6) Stephens S M Dluhy R A *Thin Solid Films* **1996** *284–285* 381
(7) Mueller H Butt H J Bamberg E *J Phys Chem B* **2000** *104* 4552
(8) Desmeules P Grandbois M Bondarenko V A Yamazaki A Sales e C *Biophys J* **2002** *82* 3343–3350
(9) Sackman E *Science* **1996** *271* 43
(10) Kaasgaard T Leidy C Ipsen J H Mouritsen O G Jorgensen K *Single Mol* **2001** *2* 105
(11) Seantier B Breffa C Felix O Decher G *Nano Lett* **2004** *4* (1) 5
(12) Slade A Luh J Ho S Yip C M *J Struct Biol* **2002** *137* 283
(13) Malmsten M *J Colloid Interface Sci* **1995** *17* 106
(14) Chapman D *Langmuir* **1993** *9* 39
(15) Ahlers M Muller W Reichert A Ringsdorf H Venzmer J *Angew Chem* **1990** *29* 1269
(16) Shannon Moore M Mahaffey D T Bradsky F M Anderson R G W *Science* **1987** *236* 559
(17) Smith D P E Bryant A Quate C F Rabe J P Cerber Ch Swalen J D *Proc Natl Acad Sci U S A* **1987** *84* 969
(18) Heim M Cevec G Cuckenberger R Knapp H F Wiegrabe W *Biophys J* **1995** *69* 189
(19) Egger M Ohnesorge F Weisenhorn A L Heyn S P Drake B Prater C B Gould S A C Hansma P K Gaub H E *J Struct Biol* **1990** *103* 89
(20) Zasadzinski J A N Helm C A Longo M L Weisenhorn A I Gould S A C Hansma P K *Biophys J* **1991** *59* 755
(21) Hansma H G Gould S A C Hansma P K Gaub H E Longo M L Zasadzinski J A N *Langmuir* **1991** *7* 1051
(22) Hansma H G Weisenhorn A I Edmundson A B Gaub H E Hansma P K *Clin Chem* **1991** *37* 1497
(23) Singh S Keller D J *Biophys J* **1991** *60* 1401
(24) Vikholm I Peltonen J Teleman O *Biochim Biophys Acta* **1995** *111* 1233
(25) Mou J Yang J Shao Z *Biochemistry* **1994** *33* 4139
(26) Mou J Yang J Huang C Shao Z *Biochemistry* **1994** *33* 9981
(27) Hui S W Viswanathan R Zasadzinski J A Israelachvili J N *Biophys J* **1995** *68* 171
(28) Israelachvili J N *Langmuir* **1994** *10* 3369

10 1021/la050644q CCC $30 25
Published on Web 06/28/2005

Although some studies of absorbed phospholipid layers on silicon nitride surfaces have shown that they are strong lubricants and appear to be crucial in joint lubrication and in the composition of synovial fluid,[30] little is known about the frictional response of SPBs. Lateral force microscopy (LFM) has been widely used in the study of the frictional and elastic properties of organic thin films and self-assembled monolayers (SAMs) of alkylsiloxanes.[31-35] It provides quantitative force measurements, thanks to the development of techniques able to calibrate the vertical[36-38] and lateral[39,40] spring constant of the probes. In the past, almost all studies involving LFM were performed in air due to the mechanical instabilities that arise when measurements are done in a liquid environment, partly due to the high density of the medium and to the turbulences that are created as the tip scans the sample. Hay et al.[41] showed that lateral force contrast could be obtained in aqueous solutions. Other authors used LFM to obtain quantitative friction measurements on different surfaces, while ramping the vertical force applied on the sample. Along these lines, Binggeli et al.[42] studied the influence of humidity on friction measurements and discussed the effect of the water meniscus that forms between the tip and the sample and Clear et al.[43] tested the frictional properties of alkanesilanes immersed in alcohols of different lengths. In the field of biological samples, Grant et al.[44] studied the mechanical properties of 1,2-dioleoyl-*sn*-glycero-3-phosphocholine (DOPC) bilayers by means of LFM and AFM vertical force spectroscopy in a liquid.

Recent theoretical calculations have revealed the critical role of NaCl in the structure of phospholipid bilayers and have shown how the phosphocholine polar heads present in some phospholipid molecules pack in a more compact way as NaCl concentration increases.[45,46] This was experimentally confirmed by our group, which performed force spectroscopy on 1,2-dimyristoyl-*sn*-glycero-3-phosphocholine (DMPC), 2-dilauroyl-*sn*-glycero-3-phosphocholine (DLPC), 1,2-dipalmitoyl-*sn*-glycero-3-phosphocholine (DPPC), and 1-palmitoyl-2-oleoyl-*sn*-glycero-3-phosphoethanolamine (POPE) and detected the force at which the phospholipid bilayer breaks as a function of NaCl concentration.[47]

The aim of the study reported here was to detect the structural changes induced by various amounts of NaCl on a DMPC bilayer by means of lateral force microscopy in a liquid environment and to give a better insight into the mechanical interaction between the tip and bilayer as friction between them is created at increasing vertical forces. One of the first studies of LFM in liquid media, it opens up a new path for studying the frictional properties of biological samples under a wide range of conditions and obtaining quantitative force values.

Experimental Section

Materials. DMPC at >98% purity was obtained from Sigma. Chloroform at >99.8% purity was obtained from Fluka and analysis-grade ethanol at 99.9% purity from Carlo Erba. Water was purified by distillation followed by deionization in an ion-exchange unit and then passage through a Milli-Q RG system consisting of charcoal filters, ion exchange media, and a 0.2 μm filter. CLLS-grade mica was obtained from Metafix (Montdidier, France).

Sample Preparation. DMPC was dissolved in chloroform/ethanol (3:1) to give a final DMPC concentration of 2 mM. This solution was maintained at −10 °C. A 500 μL aliquot was poured into a glass vial, and the solvent was evaporated with a nitrogen flow, leaving a DMPC film at the bottom of the vial. Then water was added to a final DMPC concentration of 500 μM. Because of the low solubility of DMPC in water, the vial was subjected to 30 s cycles of vortexing and sonication until a homogeneous mixture, always protected from light and maintained at 0 °C, was formed. Four aliquots of 50 μL were poured into four eppendorfs, with addition of 0.3 M NaCl aqueous solution and Milli-Q water buffered with 1,1,1-triphenyl-3,3,3-tris(*m*-tolyl)-disiloxane (TRIS; pH 7.0), to obtain 0, 0.01, 0.05, and 0.1 M NaCl solutions. Prior to use, mica surfaces were glued to Teflon disks with water-insoluble mounting wax. A 50 μL sample of DMPC and a 0 M NaCl solution were applied to cover a 0.5 cm^2 freshly cleaved piece of mica for a deposition time of 35 min. After that, the mica was rinsed three times with 100 μL of Milli-Q water. Finally, 100 μL of Milli-Q water was poured onto the mica surface, making it ready for imaging and friction experiments. The same process was applied for the rest of the DMPC−NaCl solutions, with care taken to use a rinsing and imaging medium of the same NaCl concentration as the DMPC previously poured onto mica. The liquid cell (Digital Instruments, Santa Barbara, CA) was thoroughly rinsed with Milli-Q water and ethanol and finally dried with a nitrogen flow before the start of the experiments.

AFM and LFM Measurements. All friction and topographic data presented were obtained with a Dimension 3100 atomic force microscope attached to a Nanoscope IV electronic controller (Digital Instruments). All the experiments were performed at a constant temperature of 20 °C. Previous studies show that the DMPC main-phase transition takes place around 24 °C,[48] so our measurements were performed on the gel phase. An OMCL TR400PSA (Olympus, New York) 200 μm long triangular silicon nitride cantilever backside-coated in gold was used. Its vertical spring constant was set at 0.12 ± 0.02 N/m by measuring the change in the resonant frequency of the loaded and unloaded cantilever[36] with an MFP-1D atomic force microscope (Asylum, Santa Barbara, CA). To add mass to the cantilever, 5 μm nominal radius tungsten spheres were used (Novascan, Ames, IA). The spheres were suspended in acetone, spread on a glass slide, and imaged with the optical stage of the MFP-1D. Then, one of them was picked up with the cantilever by capillarity, with avoidance of any kind of glue. This is a nondestructive method and avoids the error caused by the mass of glue applied. To achieve good results with this calibration technique, it is crucial to measure as accurately as possible the real radius of the spheres and so calculate the added mass. To get the mean radium of a tungsten particle on a glass slide, one was chosen and imaged with the MFP-1D optical stage. Because the optical stage was beneath the sample, it was possible to image the tungsten particle and the tip at the same time. Then, the particle was moved with the

(29) Yang, J.; Appleyard, J. *J. Phys. Chem. B* **2000**, *104*, 8097.
(30) Schwarz, I. M.; Hills, B. A. *J. Rheumatol.* **1998**, *37*, 21.
(31) Tian, F.; Xiao, X.; Loy, M. M. T.; Wang, C.; Bai, C. *Langmuir* **1999**, *15*, 244.
(32) Lee, B. W.; Clark, N. A. *Langmuir* **1998**, *14*, 5495.
(33) Huang, J. Y.; Sang, K. J.; Lagontchev, A.; Yang, P. K.; Chuang, T. J. *Langmuir* **1997**, *13*, 59.
(34) Xiao, X.; Hu, J.; Charych, D. H.; Salmeron, M. *Langmuir* **1996**, *12*, 235.
(35) Reiter, G.; Demirel, A. L.; Peanosky, J.; Cai, L. L.; Granick, S. *J. Chem. Phys.* **1994**. *101*, 2606.
(36) Cleveland, J. P.; Manne, S.; Bocek, D.; Hansma, P. K. *Rev. Sci. Instrum.* **1993**, *64*, 403.
(37) Ruan, J. A.; Bhushan, B. *Trans. ASME, J. Tribol.* **1994**, *116*, 378.
(38) Sader, J. E. *Rev. Sci. Instrum.* **1995**, *66* (9), 4593.
(39) Ogletree, D. F.; Carpick, R. W.; Salmeron, M. *Rev. Sci. Instrum.* **1996**, *67* (9), 3298.
(40) Sheiko, S. S.; Möller, M.; Reuvekamp, E. M. C. M.; Zandbergen, H. W. *Phys. Rev. B* **1993**, *48*, 5675.
(41) Hay, M. B.; Workman, R. K.; Manne, S. *Langmuir* **2003**, *19*, 3727.
(42) Binggeli, M.; Mate, C. M. *J. Vac. Sci. Technol., B* **1995**, *13* (3), 1312.
(43) Clear, S. C.; Nealey, P. F. *Langmuir* **2001**, *17*, 720.
(44) Grant, L. M.; Tiberg, F. *Biophys. J.* **2002**, *82*, 1373.
(45) Böckmann, R.; Grubmüller, H. *Angew. Chem., Int. Ed.* **2004**, *43*, 1021.
(46) Böckmann, R.; Hac, A.; Heimburg, T.; Grubmuller, H. *Biophys. J.* **2003**, *85*, 1647.
(47) Garcia-Manyes, S.; Oncins, G.; Sanz, F. Submitted for publicationto *Biophys. J.*

(48) Enders, O.; Ngezahayo, A.; Wiechmann, M.; Leisten, F.; Kolb, H.-A. *Biophys. J.* **2004**, *87*,0.2522.

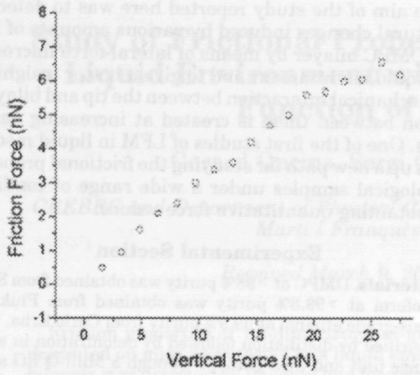

Figure 1. Friction force vs vertical force curve obtained on bare mica in Milli-Q water. Used as a reference for measurements on DMPC bilayers. The error bars represent the confidence intervals (95% CI, number of samples 256).

aim of the tip and imaged again. This process was repeated four times, giving rise to a radius variation around 10%. The mean radius was used to calculate the weight of the sphere. Then, the size of the particle was compared with the cantilever length, which had been previously measured with a BH2-UMA optical microscope (Olympus). Then, the tip was maintained in a water environment for 2 h at 20 °C before the beginning of the friction measurements until a stable reflection of the laser on the photodetector was achieved. Because of the downward bending of the cantilever on increasing NaCl concentration that was observed in preliminary experiments, the laser was initially adjusted so as to always remain reflected around the central zone of the photodiode that had been previously found by force curves to have a linear response. To prevent possible vertical and lateral photodiode sensitivity changes and to obtain comparable friction results, DMPC friction experiments and lateral calibrations were performed with the same tip, with the zone of laser incidence on the cantilever changing as little as possible. The apex of the tip was rubbed on mica before the experiments to remove asperities and to ensure a tip radius around 50 ± 10 nm. This process is crucial to obtaining reproducible results[49] and ensuring a constant tip radius during the entire experiment. Lateral sensitivity of the cantilever was calculated by scanning of $SrTiO_3$ and the method of Ogletree et al.[50] This lateral calibration was done under water, to reproduce experimental conditions as closely as possible. Between samples, the tip was rinsed with the NaCl medium of the following sample without being removed from the AFM holder, so as to maintain constant photodiode sensitivity. There was a 15 min wait before friction to let the cantilever accommodate to the new NaCl concentration. During friction experiments, the tip and the cantilever were always immersed in the aqueous medium. For the sake of simplicity, only one set of experiments is given in this paper. Reproducibility was tested with various tips and samples, and it was found that friction force reproducibility was higher (10%) for tips coming from the same batch than for different batch tips (20%). Nevertheless, the shape and general trend of the friction force vs vertical force experiments was consistent for 80% of the tested tips. All tips were worn down prior to use to a radius of 50 ± 15 nm.

Force curves were obtained at a scan rate of 1 Hz and with a Z range of 600 nm, and the raw data of detector voltage versus sample piezo voltage were converted to force displacement curves, following the method described elsewhere.[50] The gains were set at around 1–2 to ensure a constant vertical force on the layers throughout the friction loops. Friction data were obtained by averaging 256 consecutive friction loops with 512 pixels per line resolution for every vertical force value. Edges of friction loops were removed to reduce artifacts arising from the lever turning around. The lateral scanning area of every friction loop was set to 1.66 μm × 0.2 μm with a tip velocity of 19.7 μm/s. Even though the width of the friction loops proved constant for a tip velocity of 2 μm/s onward, the experiments were performed at a higher rate because of a better signal/noise ratio. In friction experiments, the vertical force 0 was defined as the force exerted on the surface by the tip when there is no signal feedback from the microscope (undistorted cantilever deflection before the sample is approached). As adhesive forces are negligible in the experiments reported in this study, negative vertical forces are not included.

(49) Qian, L.; Xiao, X.; Wen, S. *Langmuir* **2000**, *16* (2), 662.
(50) Ducker, W. A.; Senden, T. J.; Pashley, R. M. *Langmuir* **1992**, *8*, 1831.

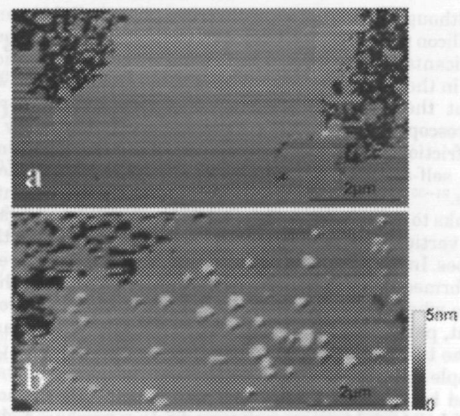

Figure 2. AFM topographic images of DMPC bilayers, 0.1 M NaCl: (a) after rinsing with 0.1 M NaCl aqueous solution; (b) without the rinsing process. Spurious contamination on the surface makes the latter unsuitable for friction measurements.

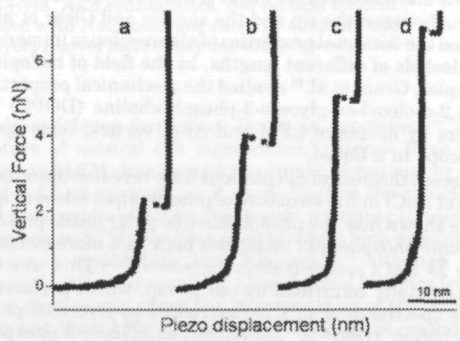

Figure 3. Penetration curve obtained on a DMPC bilayer deposited on mica at different NaCl concentrations: (a) Milli-Q water; (b) 0.01 M NaCl; (c) 0.05 M NaCl; (d) 0.1 M NaCl. The breakthrough reveals the presence of the bilayer. A more detailed statistical treatment of penetration curves obtained at different NaCl concentrations is presented elsewhere.[47]

Results

Figure 1 shows a friction experiment on clean mica in pure Milli-Q water used as a reference for further experiments on DMPC bilayers. After this, the first DMPC bilayer was formed on mica and a friction set of data was measured. As shown in Figure 2, the rinsing process prior to imaging was crucial to obtaining DMPC islands without spurious contamination and gave rise to smooth islands ca. 6 nm high.[13] For the purpose of this study, islands were more desirable than complete bilayers because the presence of holes enabled us to confirm the presence of the bilayer and measure its height. The DMPC islands were large enough to prevent the tip from testing DMPC areas near the rim of the bilayer.

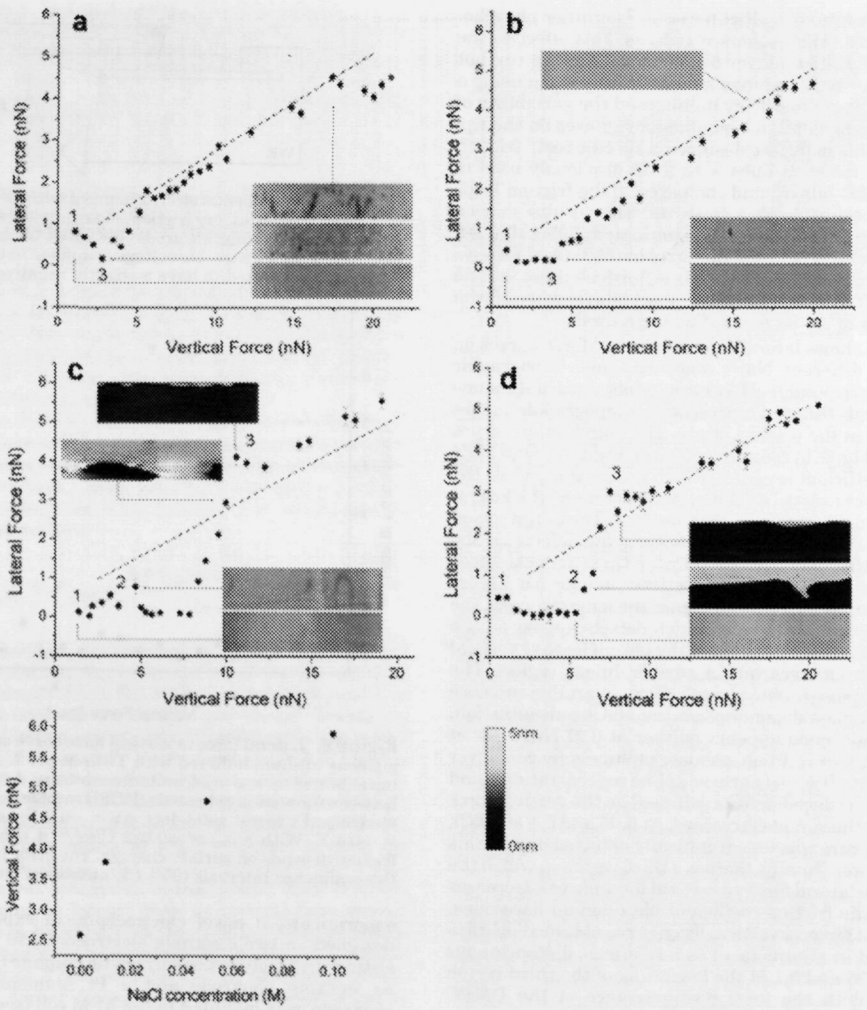

Figure 4. Lateral force vs vertical force curves on DMPC bilayers in an aqueous environment. NaCl concentration is (a) 0 M, (b) 0.01 M, (c) 0.05 M, and (d) 0.1 M. Graphs are accompanied by bilayer topographic images (1.66 × 0.2 μm) obtained simultaneously with the friction data. The error bars represent the confidence intervals (at 95%, number of samples 256). A reference lateral force vs vertical force curve obtained on mica is included in every panel (dashed line). Curves were divided into three regions, the beginning of each of which is labeled 1, 2, and 3. The first region shows an extremely low friction force because of the repulsive electrostatic interactions due to DMPC polar heads and the tip. During the second region, the tip creates defects or begins to break the bilayer and the lateral force increases steeply. The second region is not visible in curves a and b. In the third region the tip contacts the mica beneath the bilayer. (e) shows the vertical forces at which the second region begins as a function of NaCl concentration.

As shown previously,[7,43,51] bilayers break under the pressure exerted by the tip, giving a typical discontinuity in the indentation curve known as "breakthrough". Figure 3 shows a set of penetration curves registered on DMPC islands at different NaCl concentrations. A sudden indentation jump in these curves means that the DMPC bilayer breaks under the pressure exerted by the tip. As can be seen, the breakthrough force increases with the NaCl concentration. This fact will be considered in more detail in the Discussion and in a future paper,[47] in which the effect of ionic strength on the mechanical stability of phospholipid bilayers will be studied by force spectroscopy.

After breaking of the bilayer, there is a hard-wall contact between the tip and the mica, which is seen in the penetration curves as a very steep region after the breakthrough. Penetration curves were also obtained to check the appropriate vertical force range for friction measurements, because they show the vertical force at which the bilayer is punctured and give an idea of the force at which the bilayer breaks during lateral force vs vertical force curves. The breakthrough distance is ~5 nm (comparable to the width of the DMPC bilayer), although the distance between the beginning of the repulsive zone and the hard-wall contact is greater than the height of the DMPC bilayer. This effect has been

(51) Schneider, J.; Barger, W.; Lee, G. U. *Langmuir* **2003**, *19*, 1899.

reported previously by Richter et al.[52] for other phospholipid systems. The authors attributed this effect to the *presence of a lipid bilayer on the surface of the tip*, but Franz et al.[53] only obtained similar results when using a tip with a big radius. They highlighted the variability of the tip coverage and phospholipid structures on the tip. To clarify this point, we designed a specific test: friction loops were made on mica with a tip previously used to scan a DMPC bilayer and compared to the friction loops on mica obtained with a fresh tip. The results showed that, although there was a contamination effect that led to random deviation from linearity in the lateral force vs vertical force graphs, under our conditions there was no evidence of the formation of a compact bilayer when silicon nitride tips of ca. 50 nm radius were used.

Figure 4 shows lateral force vs vertical force curves on DMPC at different NaCl concentrations. Topographic images shown beside each curve were obtained at the same moment. Only the most representative topographic images are shown in the present study. The four friction curves in Figure 4 have in common an initial region in which the friction coefficient is near 0, which means that, while the vertical force exerted on the sample increases, the lateral force response remains almost constant. The initial region ends with the appearance of topographic defects on the surface of the bilayer, created by the tip at vertical forces of 2.6, 3.8, 4.8, and 5.9 nN, respectively, as shown in Figure 4e. It is clear, then, that the higher the ionic strength, the higher the vertical force at which defects appear on the bilayer. After this, the shape of the lateral force vs vertical force graph changes into a steeper linear region. The associated topographic images show a variable increase of layer damage depending on the NaCl concentration. This second region appears neither at 0 M NaCl nor at 0.01 M NaCl. In addition, no topographic evidence of layer rupture was observed at these saline concentrations, and most of the induced defects self-heal as the vertical force applied on the sample increases. At 0.05 and 0.1 M NaCl, bilayer rupture was topographically detected during this second region. Finally, there is a third region in which the slope of the lateral force vs vertical force curves decreases to match the friction coefficient obtained on bare mica. The lateral force vs vertical force curve obtained on mica is included in Figure 4a–d as a reference discontinuous line. At 0.05 and 0.1 M the beginning of the third region coincides with the total disappearance of the DMPC bilayer, as shown on the topographic images.

Bilayer defects were observed at 0, 0.1, and 0.5 M NaCl and appeared at higher vertical forces as ionic strength increased. No sign of defects was found in the bilayer of Figure 4d. According to the response of DMPC against vertical force exerted by the tip, the bilayers of Figure 4a,b (low NaCl concentration) recovered from defects and poor or null propagation of them was found, while the Figure 4c,d curves display bilayer breaking and no recovery capacity. The increment of vertical force from the beginning of the second region to the beginning of the third region is 3.5 nN in the bilayer of Figure 4c and 1.2 nN in the bilayer of Figure 4d. As a consequence, the transition between the near 0 friction regime (first region) and the contact between the tip and mica (third region), when it exists, becomes shorter as the NaCl concentration increases.

To ensure that electrostatic repulsion reduces lateral force almost to 0 nN, as in the first region of the friction

(52) Richter, R. P.; Brisson, A. *Langmuir* **2003**, *19*, 1632.
(53) Franz, V.; Loi, S.; Muller, H.; Bamberg, E.; Butt, H. *Colloids Surf., B* **2002**, *23*, 191.

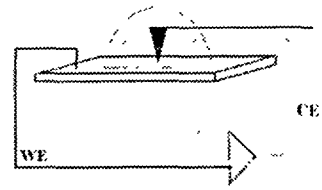

Figure 5. Experimental electrochemical setup to test the effect of charged surfaces on friction measurements in a liquid environment: working electrode (WE), HOPG surface; counter electrode (CE), Pt wire. No voltage is applied to the tip. At pH 7, the tip is expected to have a slightly negative charge.[36]

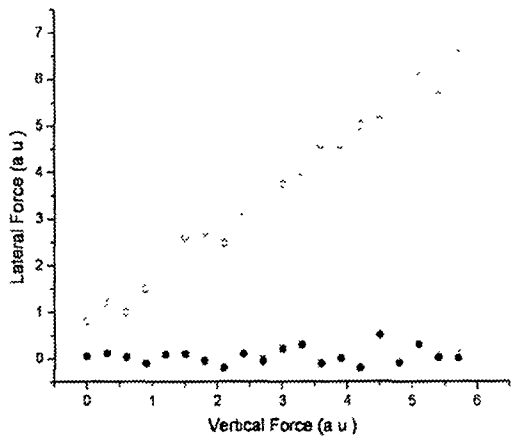

Figure 6. Lateral force vs vertical force curve on HOPG in an aqueous medium buffered with TRIS at pH 7. As a different uncalibrated tip was used, units are arbitrary. A ΔV was applied between the working electrode (HOPG sample) and the counter electrode (Pt wire): solid dots, $\Delta V = -0.3$ V; empty dots, $\Delta V = +0.3$ V. With a σ_{ox} of -0.032 C/m^2,[36] it can be seen that friction depends on surface charges. The error bars represent the confidence intervals (95% CI, number of samples 256).

experiments, a novel electrochemical experiment was designed: a two-electrode electrochemical system, consisting of a highly ordered pyrolytic graphite (HOPG) sheet as working electrode and a Pt filament as counter electrode, was mounted in the AFM cell (see Figure 5 for the experimental setup) and immersed in TRIS-buffered water at pH 7. Potentials of 0.3 and −0.3 V were applied to the HOPG, and lateral force vs vertical force curves were recorded (Figure 6). As a silicon nitride tip has a slightly negative charge,[36] friction can be modulated as a function of the surface charge and the lateral force can be reduced to nearly 0 when the tip and sample charges have the same sign. It is important to note that, in this electrochemical setup, the tip was not connected to any electrode, so its charge remained constant during the entire experiment. As no reference electrode was mounted in the electrochemical cell, voltages applied are not absolute values.

Discussion

This study corroborates the findings of Grant et al.[41] *about the mechanical behavior of phospholipid bilayers* (DOPC in their case) in a liquid environment. It used force spectroscopy and friction measurements and provides new insights into lateral force vs vertical force curves. The first region consists of a soft contact between the lipid bilayer deposited on mica and the tip. As can be seen in

Table 1. Calculus of σ_{DMPC} for Every NaCl Concentration, Applying DLVO Theory, for a Contact between Planar and Spherical Charged Surfaces[a]

NaCl concn (M)	F_{DLVO} (nN)	DMPC charge density (C/m^2)	no. of Na$^+$ ions per DMPC molecule
0.01	3.8	−0.06	0.2
0.05	4.8	−0.18	0.6
0.1	5.9	−0.34	1.0

[a] F_{DLVO} is taken as the vertical force at which the first lateral force vs vertical force curve region ends. A 0.5 nm^2 area per DMPC molecule is assumed. The ratio of Na$^+$ ions per DMPC molecule is given.

Figure 3, there is a repulsive zone at the beginning of the contact region of the approaching force curve that can be related to the first region obtained in the friction curves shown in Figure 4. At low vertical loads, the tip and the surface show extremely low friction due to a repulsive electrostatic interaction.

To understand why the first region (electrostatic repulsion) in the lateral force vs vertical force curves broadens as NaCl concentration increases, Derjaguin–Landau–Verwey–Overbeek theory (DLVO[51]) was applied. When interaction is between a flat (sample) and a hemispheric (tip) charged surface

$$F_{DLVO} = F_{elec} + F_{VdW} = \frac{4\pi\sigma_{DMPC}\sigma_{tip}R_{tip}\lambda}{\epsilon_0\epsilon}e^{-z/\lambda} - \frac{H_A R_{tip}}{6z^2}$$

where σ_{DMPC} and σ_{tip} are the surface charges of the DMPC bilayer and the tip, R_{tip} is the radius of the tip, and λ is the Debye length. H_A is the Hamaker constant, and z is the distance between the sample and the tip. Taking an H_A of 10^{-21} J (value calculated for hydrocarbons in water by Butt et al.[52]), a σ_{tip} of −0.032 C/m^2 at pH 7.0,[53] and a mean area per molecule of 0.5 nm^2,[54] we obtain the σ_{DMPC} values for the different saline concentrations tested. As a first approximation and to obtain qualitative results about the surface charge of DMPC bilayers at different NaCl concentrations, the F_{DLVO} necessary for these calculations was considered as the vertical force at which the first region in lateral force vs vertical force curves ends, which is believed to be the vertical force at which the bilayer begins to be damaged by the tip. As has been seen in Figure 3, penetration curves present a breakthrough at higher forces when NaCl concentration is increased, so friction results seem to complement this fact. It is important to note that this is a first approximation in which the mechanical strength of the bilayer is reduced to an electrostatic interaction between the bilayer and the tip. Future research by our group will focus on clarifying this assumption. Results are shown in Table 1. Some recent simulation results on POPC[56] show how Na$^+$ can position in a tridentate way between PO_4^- groups in POPC polar heads. As POPC and DMPC polar heads are identical, it is reasonable to suppose that Na$^+$ will penetrate DMPC polar heads in a similar way. Results shown in Table 1 are consistent with the Na$^+$/phospholipid ratio proposed[45,56] and show that σ_{DMPC} probably changes as NaCl concentration increases.

The second region of the lateral force vs vertical force curves shows a steep increase in friction coefficient (Figure 4). As shown in previous studies, a great increase in friction

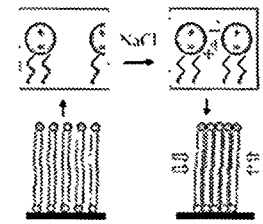

Figure 7. Effect of NaCl in DMPC molecule packing. The circles represent the DMPC polar heads and the zigzag lines the hydrocarbon chains. Without NaCl, electrostatic repulsion arising from the charge distribution of DMPC polar heads decreases bilayer compactness. When NaCl is provided, DMPC polar head charges are screened and bilayer compactness increases.

may be due to disorder or to the lack of cohesion and packing of the sample.[5,8,55] The topographic images in Figure 4 show that, in this second region, defects or breaks are induced on the DMPC bilayer because of the vertical force applied by the tip. As a consequence, we believe that the loss of structure in the bilayer is responsible for the steep friction increase and that in this region there is a mechanical transition of the tip from the bilayer surface to the mica surface. At the end of this transition, the third region begins. As highlighted previously, the friction coefficient of the third region of the lateral force vs vertical force curves is very similar to that obtained for bare mica, so we propose relating it to a hard-wall contact between the mica and the tip. This means that, in this third region, the vertical force applied by the tip is enough to remove the DMPC bilayer from the surface of the mica.

Interestingly, the vertical force range of the first and second regions of the lateral force vs vertical force curves varies greatly with NaCl concentration. This can be explained with the model shown in Figure 7. As DMPC polar heads are zwitterionic, they show separation of charges though they are neutral overall. When there is no electrolyte in solution, DMPC individual molecules do not pack as efficiently as possible due to electrostatic repulsion between polar heads (Figure 7). This leads to less cohesion in bilayers when NaCl concentration is low. This is shown in Figure 4, in which the end of the lateral force vs vertical force curves in the first region shifts to higher vertical forces when NaCl concentration increases. A greater distance between molecules implies lower cohesive energy and a more fluent structure. In addition, low-NaCl-concentration bilayers show defects that tend to disappear or not to grow while vertical force increases. This can be explained by assuming that DMPC molecules restructure to replace the molecules removed by the tip during friction experiments (Figure 8a). No bilayer breakage is noticed topographically because the structure is fluid enough for the molecules to rearrange under the pressure exerted by the tip, filling the holes created after tip scanning. When NaCl concentration increases, ions screen the charge of the polar heads, letting DMPC molecules pack in a tighter structure and leading to more rigid bilayers unable to restructure. For this reason, defect concentration is lower and layer breakage is noticed (Figure 8c,d). A recent study proved that the self-diffusion of a phosphocholine-terminated phospholipid decreases with increasing ionic concentration,[57] which corroborates the decrease in self-healing capacity shown in this study.

(54) Israelachvili, J. *Intermolecular Surface Forces*, 1991.
(55) Butt, H.-J., Jaschke, M.; Ducker, W. *Bioelectrochem. Bioenerg.* **1995**, *38*, 191.
(56) Butt, H.-J. *Biophys. J.* **1991**, *60*, 1438.
(57) Tristram-Nagle, S.; Liu, Y.; Legleiter, J.; Nagle, J. *Biophys. J.* **2002**, *83*, 3324.
(58) Kim, H. I.; Graupe, M.; Oloba, O.; Koini, T.; Imaduddin, S.; Lee, R.; Perry, S. *Langmuir* **1999**, *15*, 3179.
(59) Kim, H. I.; Koini, T.; Lee, R.; Perry, S. *Langmuir* **1997**, *13*, 7192.

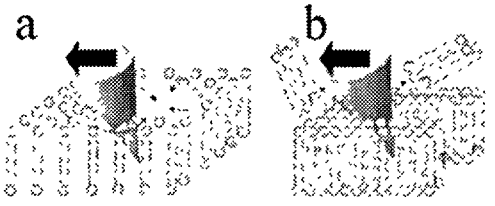

Figure 8. Mechanical interaction between the tip and the DMPC bilayer during friction experiments in a liquid environment. (a) In pure water or at low NaCl concentration, DMPC molecules restructure due to their high mobility when the bilayer is ruptured by the tip in friction experiments. (b) At high NaCl concentration, bilayer compactness and its resistance to being punctured by the tip increase.

Measurements performed at 0.05 M give a transition concentration, at which the bilayer is soft enough to have defects and hard enough to show bilayer breaks when imaged topographically. The model presented in this study to explain the increased mechanical stability of DMPC bilayers with NaCl was recently pointed out by Pandit et al.,[59] who proved that the binding of Na^+ and Cl^- to a phosphatidylcholine membrane leads to a more compact bilayer structure. These data were supported experimentally and with MD simulations, showing that not only the headgroups but also the hydrocarbon tails pack in a tighter structure as NaCl concentration increases. Along these lines, Böckmann et al.[16] proved through MD simulations that there is a strong interaction between sodium ions and the carbonyl oxygens of the lipids, which could account for the increased mechanical stability of phosphocholine bilayers in the presence of ions.

(59) Pandit, S. A.; Bostick, D.; Berkowitz, M. L. *Biophys. J.* **2003**, *84*, 3743.

Conclusion

DMPC-supported planar bilayers were prepared on mica in aqueous environments ranging from Milli-Q water to 0.1 M NaCl. LFM was used to obtain DMPC bilayer lateral force vs vertical force representations, while topographic images were obtained simultaneously. Three regimes were found in lateral force vs vertical force graphs: first, a region of extremely low friction that was related to electrostatic repulsion between the tip and DMPC polar heads, second, the response of the tip while breaking the DMPC bilayer, and, third, the hard-wall contact between the tip and the surface of the mica beneath the bilayer. At low NaCl concentrations, the DMPC bilayer is easily punctured and the tip contacts the mica at low vertical loads. As NaCl concentration increases, higher vertical forces are needed to puncture the bilayer and there is a transition between the low-friction regime and the contact with mica. This transition was detected topographically and related to the rupture of the DMPC bilayer.[47] NaCl modified the compactness of DMPC bilayers. When NaCl concentration is low, charge separation in DMPC polar heads leads to repulsion between molecules and to easily punctured bilayers. When NaCl concentration increases, charges are screened by Na^+ and Cl^- ions, leading to more compact bilayers that are difficult to puncture.

Acknowledgment. G.O. thanks the University of Barcelona for a personal grant and the DURSI (Generalitat de Catalunya) for financial support through Project 2001SGR00046. We are also grateful to Dr. Peter DeWolf, Dr. Samuel Lesko (Digital Instruments), and Matt Brukman (University of Wisconsin) for discussions about in-depth details concerning lateral force microscopy.

LA050641Q

5.4.4 Nanomechanical Properties of Supported Lipid Bilayers studies by Force Spectroscopy

S. Garcia-Manyes, G. Oncins, F. Sanz

CREBEC and Department of Physical Chemistry, Chemistry Faculty, University of Barcelona, Martí i Franquès 1-11, 08028, Barcelona Spain

Proceedings of SPIE.- The International Society for Optical Engineering (2007), 6413 (Smart Materials IV), 64130E/1-64130E/11

5.4.4.1 Summary

This work is a summary of the results presented in sections 5.4.1, 5.4.2 and 5.4.3 concerning phospholipid bilayers structure, nanomechanics and deposition process.